

Part IV
Other fibre studies

15

Introduction

In Parts II and III we have described six well-defined and different modes of tensile failure (classes 1–6 in Fig. 1.5) and four well-defined modes of fatigue failure (classes 8–11 in Fig. 1.5), together with surface wear and some examples of effects of shear splitting and peeling (classes 12 and 13 of Fig. 1.5). All of these results were obtained from simple laboratory tests on single fibres, which were mostly the widely used types of man-made fibre.

In this part there is a more diverse collection of breaks involving chemical degradation (including class 7 in Fig. 1.5), other forces such as twisting and cutting, effects of heat on fibres, natural fibres producing a variety of forms of break, and finally breaks in a variety of specialized fibre types.

16

DEGRADED FIBRES

Fibres are, in varying degrees, subject to attack by light, heat and chemicals. These agents may break polymer molecules or cause other changes in structure and thus weaken and degrade the fibre. In this chapter the effects of degradation on forms of breakage will be explored.

Nylon fibres lose strength on exposure to light, but even before there is any substantial reduction in tenacity the form of break changes. With exposure to moderate sunlight (a Manchester summer!) for 2 days, some voids show up in the V-notch region of a ductile fracture, **16A(1)**; after 3 weeks the simple V-notch and catastrophic region have both become strongly fragmented, **16A(2)**; and after 24 weeks the original form has almost completely disappeared, and the break has become a collection of separate turrets, **16A(3)**. Even with this complete change of the appearance of the break, the loss of strength is less than 10%.

Close examination, **16A(4)**, shows that each turret, or part of a turret, is associated with a conical cavity, where break has occurred. At the base of many of the cavities, a delustrant titanium dioxide particle can be seen. During drawing of the fibre, elongated (cigar-shaped) voids form round the particles, and these become enlarged by the photodegradation of the nylon, which is promoted by the TiO_2 . Under sufficient tensile stress the voids become sites for the development of ductile failure with cracks round the edge of each void opening out to give cone-shaped cavities, similar to the single internal cones shown in **5D(1),(2)**. Eventually, catastrophic failure starts, and the multiplicity of internal conical failure regions join up. The sequence is illustrated schematically in Fig. 16.1. Since the mechanics differs only in that the crack and deformation mechanism is spread over many sites rather than being concentrated in one position, the strength is not much reduced.

Prolonged exposure to intense sunshine does reduce the strength to very low values, and although the same void mechanism can be seen to be operative the appearance of the break shows that the fibre is very heavily degraded, **16A(5),(6)**, with the surface cracking of the filaments and longitudinal splits giving staggered breaks.

In bright nylon fibres, which do not contain delustrant particles, the breaks with many turrets do not occur, although the rupture is often staggered at several levels.

Thermal degradation of nylon and polyester when heated in air, so that oxidation can occur, usually changes the form of break from the ductile fracture shown in Chapter 5 to the granular form shown in Chapter 8. Examples are **16B(1)–(3),(6)**. Sometimes, **16B(1)**, the

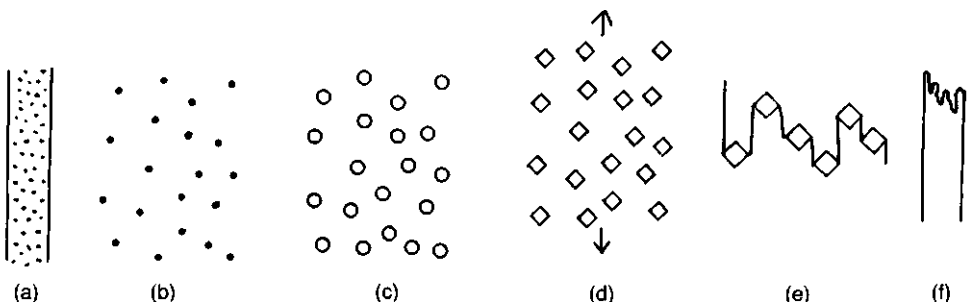


Fig. 16.1 — (a) Nylon fibre containing titanium dioxide particles. (b) Enlarged view of portion of fibre. (c) After exposure to light, voids are enlarged. (d) Cracks form under tension and lead to internal cones. (e) Cracks go catastrophic, and join up to give final break. (f) Broken fibre shows series of turrets.

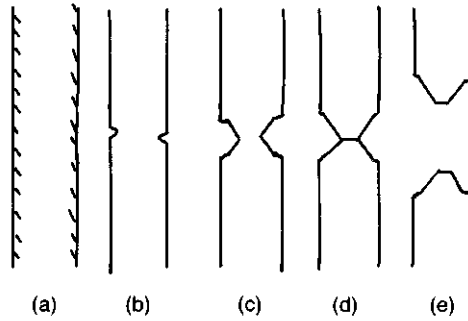


Fig. 16.2 — (a) Fibre with chemical degradation in surface layer. (b) Under tension, surface layer breaks. (c) Ductile crack develops all round fibre. (d) Catastrophic rupture at centre. (e) Broken fibre ends.

degrading action can be seen to be penetrating inwards from the fibre surface; and, in other examples, **16B(2),(3)**, there is a residual indication of an initiation region of the fracture at a point on the fibre surface. However, the granular form is not always found: in some examples, **16B(4),(5)**, the break is glass-like, suggesting a brittle failure. More research is needed to establish the circumstances which determine the form of failure, and the reasons for it.

Relatively mild oxidative action on nylon by means of a chemical environment can have an effect similar to heat, **16C(1)**. The immediate surface layer is most strongly attacked, and the form of break suggests that it fails first in a granular mode, and that this provides the initiation for crack propagation to develop as a ductile fracture in a circular notch all round the fibre, with the final catastrophic region forming the centre of the break, as illustrated in Fig. 16.2.

More severe forms of chemical attack, as illustrated in polyester in **16C(2)**, cause obviously greater damage to the fibre. The magnitude, character and effects of the reactions between a vast range of chemicals and different fibres under different conditions is a major subject which goes beyond the scope of this book, and these two pictures of tensile breaks are merely given as examples of what can happen.

Alternatively to chemical action followed by mechanical action, the two can be combined if a fatigue test, or a dead-weight loading, is carried out in a hostile environment. For example, the biaxial rotation fatigue life of nylon in hydrochloric acid or caustic soda is almost independent of pH for values greater than 2, but drops sharply below 2. Examples of the forms of break found in the biaxial rotation fatigue test under different liquid and gaseous environments are shown in **16C(3)–(6)**. The polyester fibre in nitric acid, **16C(3)**, is little affected in the appearance of break and only suffers a 10% reduction in fatigue life, but nylon in weaker nitric acid solution **16C(4)** shows a more distinct change of appearance, compared to **13D(3)**, and the fatigue life has fallen by 60%. Nitrogen dioxide also has a more severe effect on nylon, **16C(6)**, where the fatigue life has fallen from over 10000 cycles without NO_2 to 200 cycles with NO_2 , than in polyester, **16C(5)**, where the fatigue life remains over 1500 cycles.

There is one very distinctive form of fibre fracture which has only been observed after chemical attack on fibre assemblies. It was first noted by Martin Ansell at the University of Bath, and was subsequently found in a case study at UMIST, discussed in Chapter 34, **34G**. Two of Ansell's pictures are shown in **16D(1),(2)**, and others are shown in **26(B)**, where they are discussed as an example of testing a composite material. Briefly, they are tensile breaks from a PVC-coated polyester fabric which has been boiled in water for a long time. There is degradation of a surface layer, similar to that in **16C(1)**, but the break inside this layer occurs by a conical split running into the fibre, to give what has been called a stake-and-socket break, and is type 7 in Fig. 1.5. This form of axial split must be a result of shear stress, acting in the way indicated in Fig. 16.3.

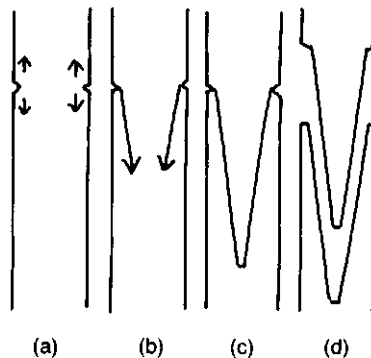


Fig. 16.3 — (a) Initial break in degraded surface layer, with shear stress at tip. (b) Shear crack propagation. (c) Completion of break. (d) Two ends of stake-and-socket break.

Finally, in this chapter, we give four examples of the effect of irradiation from work at the University of California. Moderate proton-irradiation on nylon 6 causes a partial change from ductile to granular break, **16D(3)**, but a more severe dose leads to a brittle fracture, **16D(4)**. Moderate gamma-irradiation causes most change in a surface layer, **16D(5)**, which penetrates deeper with a more severe dose, **16D(6)**.

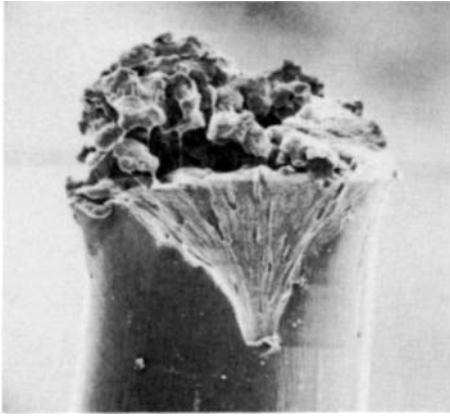
The stake-and-socket form of rupture was first found by Ansell (1983) as a result of chemical and thermal attack in PVC-coated polyester fabric, **16D(1),(2)** and **26B(3)–(6)**, then in autoclaved laboratory overalls, **34G**, in hair, **19J(1),(2)**, and in a nylon rope, **39J(1),(2)**. In none of these was the chemistry of the attack well defined. The ‘cathedral spire’ breaks of hair after exposure to ultra-violet radiation, **19J(1),(2)**, were an example of controlled laboratory testing, and stake-and-socket breaks have also now been found in laboratory studies of polyester fibres.

Holmes (1996) aminolyzed polyester fibres by treatment with *n*-butylamine in both aqueous and vapour form. The amine penetrates the fibre and breaks polymer chains, particularly extended chains in amorphous regions. Due to the action of internal stresses on the weakened material, cracks develop after prolonged exposure to amine, but these are axial cracks after vapour exposure and radial cracks after aqueous exposure. Following 192 hours in *n*-butylamine vapour, both molecular weight and strength had fallen to about 20% of the values in the original fibres. In aqueous amine the drop was only about half as much. When a vapour aminolyzed polyester fibre is extended, both axial and radial cracks are found in the outer layers, **16E(1)**, and then pieces break away, **16E(2)**. A tensile break of a fibre exposed to vapour for 144 hours shows the characteristic stake-and-socket form, **16E(3),(4)**, though this is less well developed in a fibre exposed to aqueous amine, **16E(5),(6)**, which also does not show any long axial cracks.

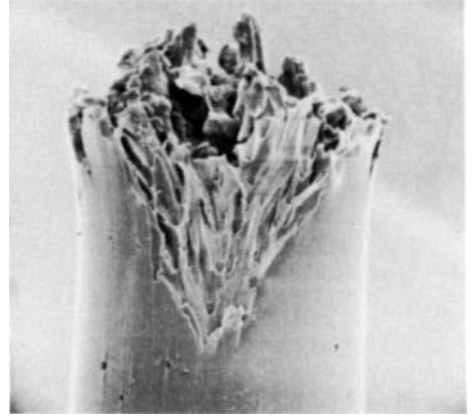
A variety of complicated forms of failure of polyester fibres, free of UV stabilizer, after exposure to ultra-violet radiation alternating with humidification have been found in studies by Salem and Ruetsch (1997). The form of break depends on the spinning conditions and consequently the resulting fibre structure. In a conventionally spun and drawn fibre, radial microcracks develop in the outer layer, **16F(1)**, but then axial and slightly off-axis cracks develop and lead to rupture, as seen in **16F(2)**. The detail may show even more complex shattering, **16F(3),(4)**.

An undrawn fibre, spun at 1500 m/min, also shows radial cracks, but these lead to smooth brittle fractures, **16F(5)**. An oriented, but high extension, fibre, spun at 5500 m/min shows shear-induced splits, **16F(6)**, and may also have some transverse cracks, giving a stepped break, **16G(1)**. Skin-core fractures, with multiple splitting in the core, are found in fibres spun at 7000 m/min, **16G(2),(3)**; similar fibres after heat-setting have the forms of damage seen in **16G(4)–(6)**. Since these fibres do not contain delustrant particles, they do not show the turreted forms found in light-degraded nylon, which were shown in **16A**.

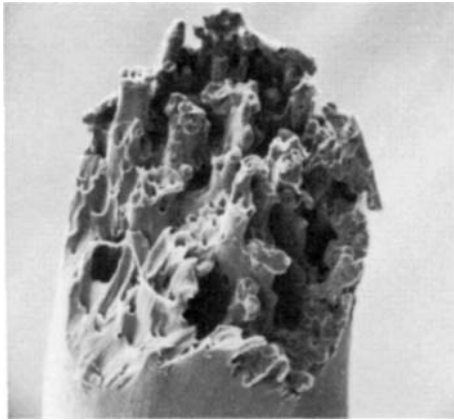
The degradation of wool by ultra-violet light has been examined by Diane Jones at UMIST. **16H(1)** shows the surface of an unexposed wool fibre. After exposure to UV for 208 Xenotest hours, **16H(2),(3)**, there is considerable damage to the fibre surface, including loss of scale definition, pitting and accumulation of debris. The tensile break of unexposed wool, **16H(4)**, is simpler than that of wool exposed to UV for 52 hours, **16H(5),(6)**, which shows an apparent loss of intercellular adhesion.



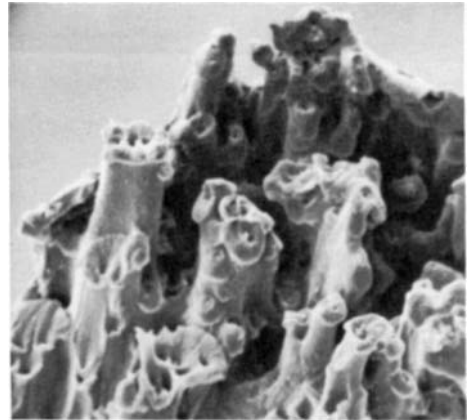
1

 10 μm


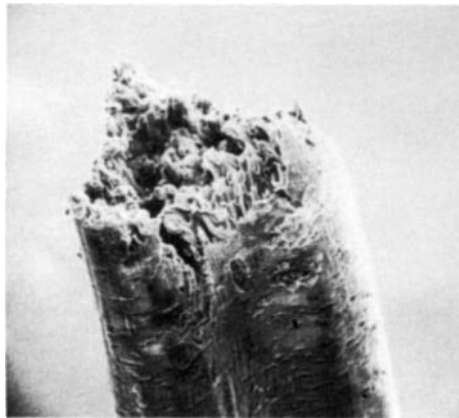
2

 10 μm


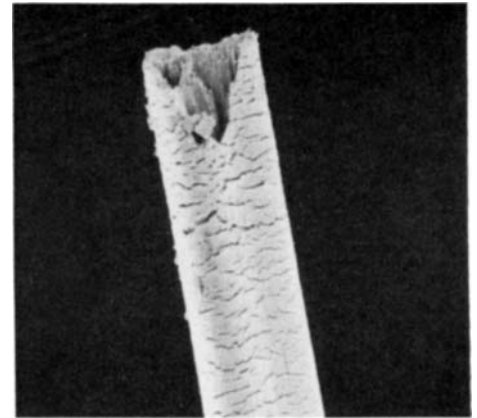
3

 10 μm


4

 5 μm


5

 10 μm


6

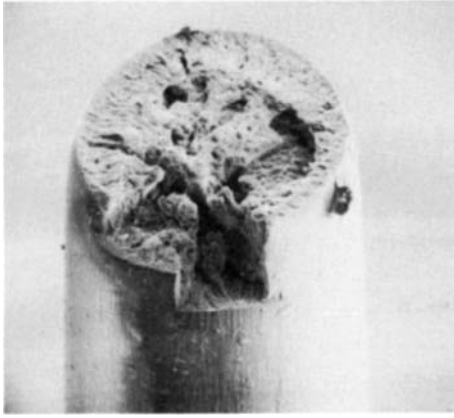
 10 μm

Plate 16A — Tensile breaks of light-degraded nylon 66, 17dtex, exposed in summer in Manchester, facing WSW.

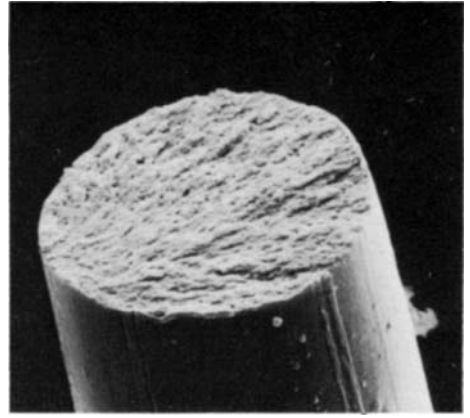
(1) 2 days exposure. (2) 3 weeks exposure. (3),(4) 24 weeks exposure.

Light-degraded trilobal nylon 66, exposed in Florida.

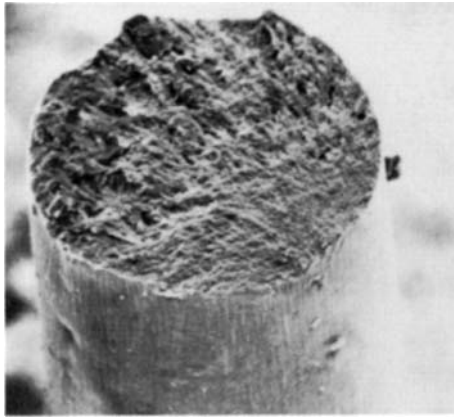
(5) 6 months exposure (600 hours of sunlight). (6) 12 months exposure (1000 hours of sunlight).



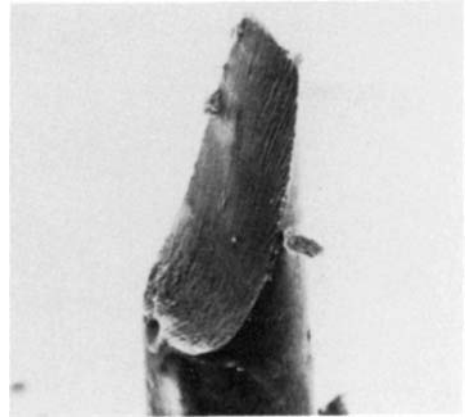
1

 10 μm


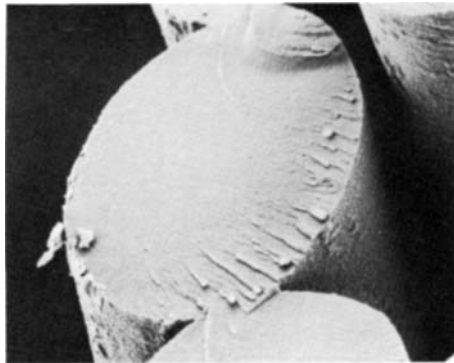
2

 5 μm


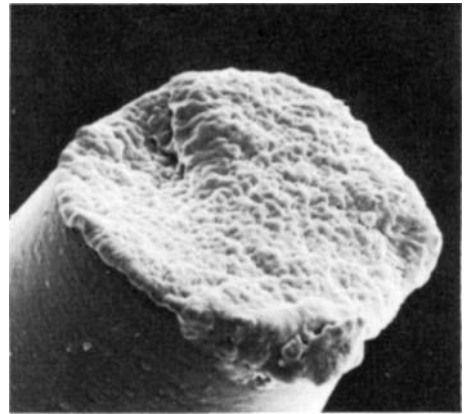
3

 5 μm


4

 10 μm


5

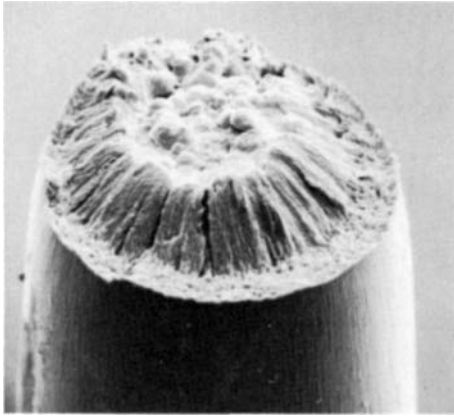
 10 μm


6

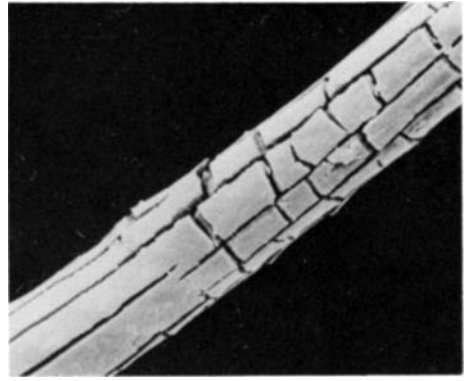
 5 μm

Plate 16B — Tensile breaks of heat-treated nylon and polyester.

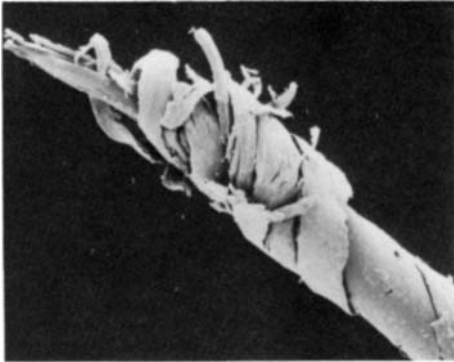
(1) Nylon 66, heated slack for 4 hours at 150°C. (2) Nylon 66, heated slack for 6 hours at 230°C. (3),(4) Nylon 66, heated slack for 4 hours at 225°C. (5) Polyester, heated slack for 6 hours at 230°C. (6) A different type of polyester fibre, heated slack for 6 hours at 230°C.



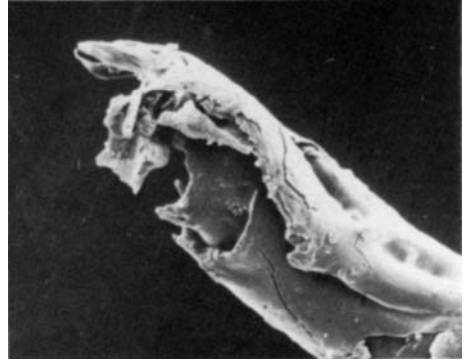
1

5 μm 

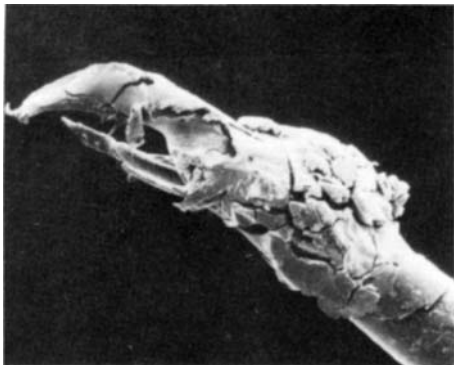
2

10 μm 

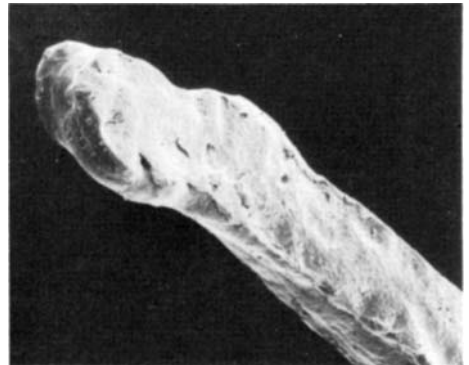
3

20 μm 

4

20 μm 

5

20 μm 

6

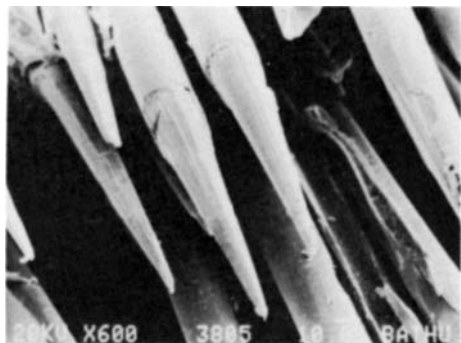
20 μm

Plate 16C — Tensile breaks of chemically degraded fibres.

(1) Nylon 66, exposed to 100 vol. H_2O_2 for 2 hours. (2) Polyester treated with *n*-propylamine for 24 hours at 25°C plus 7 hours at 40°C.

Biaxial rotation fatigue in a hostile environment.

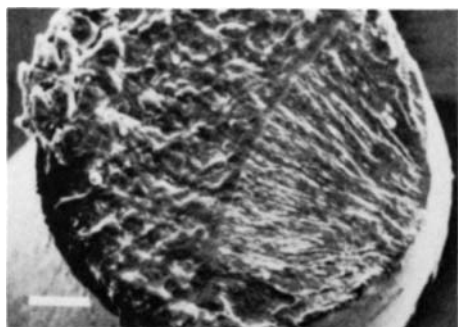
(3) Polyester in 1M HNO_3 . (4) Nylon in 0.1M HNO_3 . (5) Polyester in air + NO_2 . (6) Nylon in air + NO_2 .



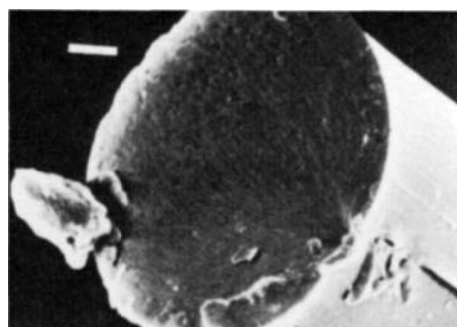
1

 20 μm

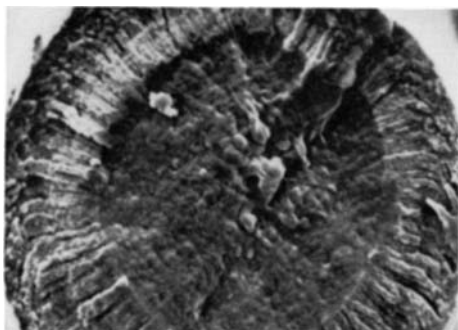

2

 10 μm


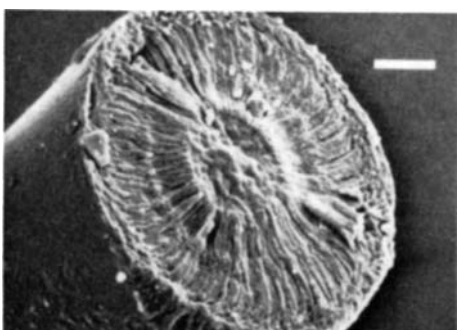
3



4



5



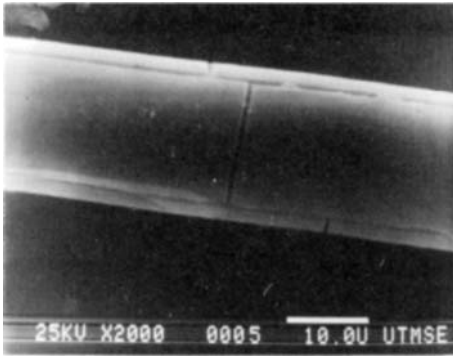
6

Plate 16D — PVC-coated polyester fabric, boiled for 6 weeks, and broken in tension (from Ansell, 1983).

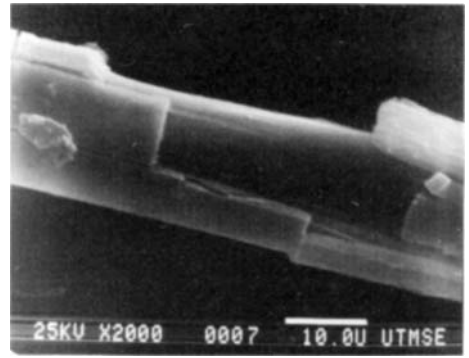
(1) Conical ends of stake-and-socket fibre fractures. (2) Fibre sockets on other end.

Tensile breaks of nylon 6 fibres after exposure to radiation (from Ellison, Zeronian and Fujiwara, 1984).

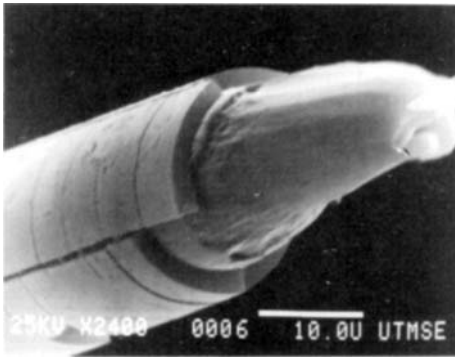
(3) After 12 Ci proton-irradiation dose. (4) After 76 Ci proton-irradiation dose. (5) After 10 Mrad gamma-irradiation. (6) After 50 Mrad gamma-irradiation.



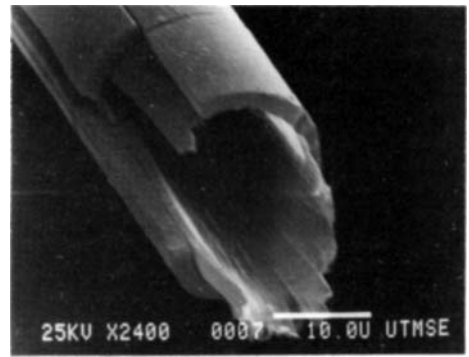
1



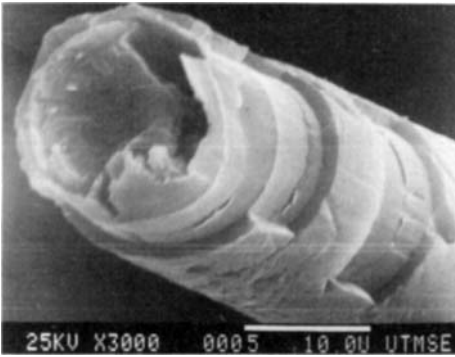
2



3



4



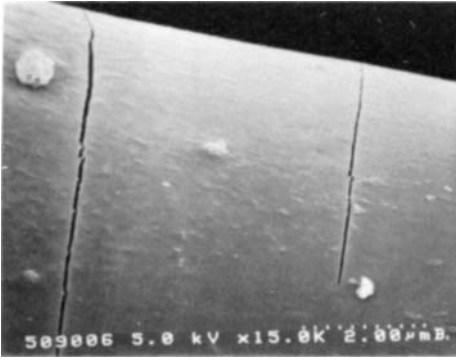
5



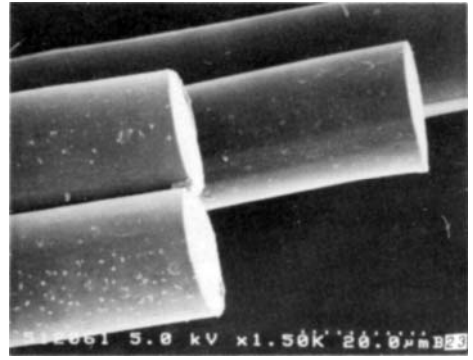
6

Plate 16E — Aminolysis of polyester fibres, Holmes (1996).

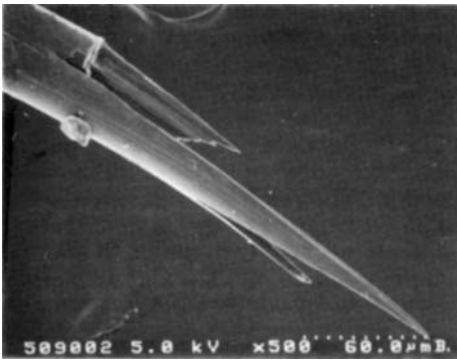
(1) Fibre exposed to *n*-butylamine vapour for 144 hours and extended to 60% of break load. (2) Taken to 75% of break load. (3),(4) Opposite ends of tensile failure after 144 hours exposure to vapour. (5),(6) Opposite ends of break of fibre exposed to aqueous amine for 144 hours.



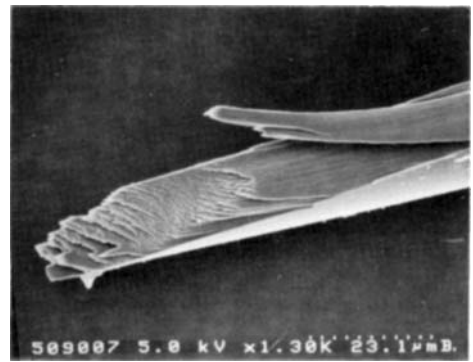
1



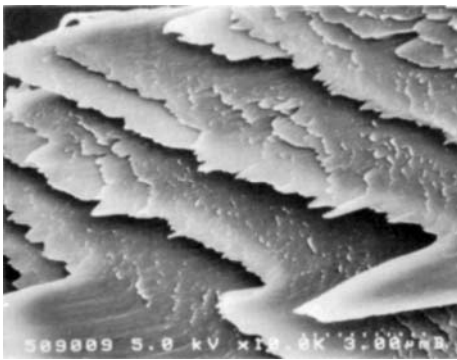
2



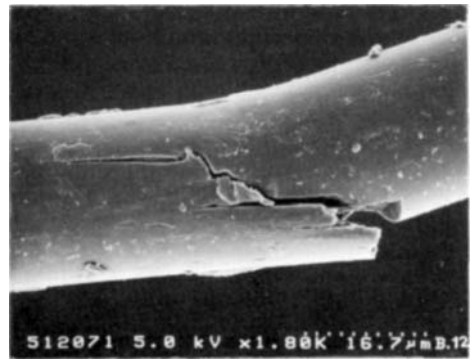
3



4



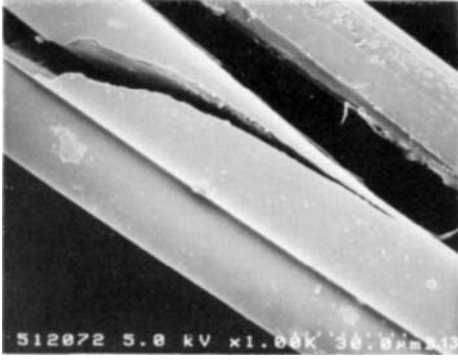
5



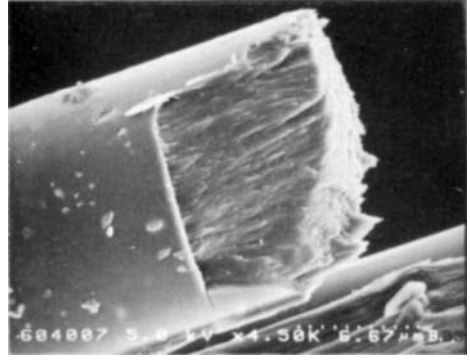
6

Plate 16F — Effects of ultra-violet exposure on tensile fractures of polyester fibres, courtesy of D. Salem and S. B. Ruetsch, TRI, Princeton.

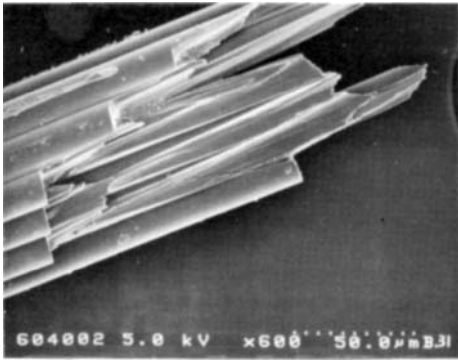
(1)–(4) High molecular weight fibre, conventionally spun and drawn. (5) Fracture of undrawn textile molecular weight fibre spun at 1500m/min. (6) Shear fracture of textile molecular weight fibre spun at 5500m/min. All after alternating exposure to UV and humidification.



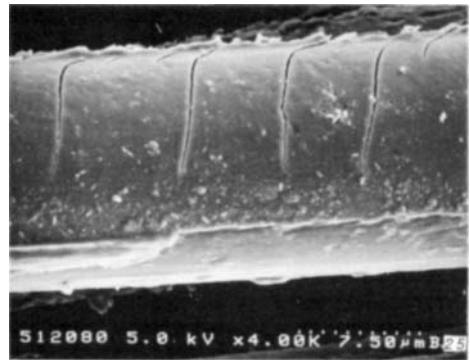
1



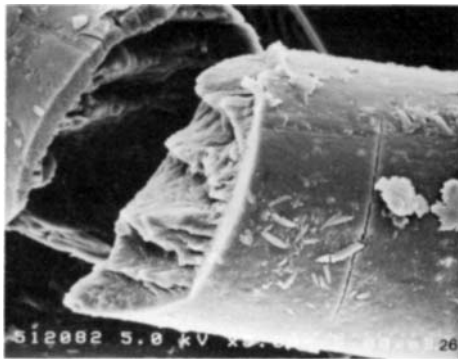
2



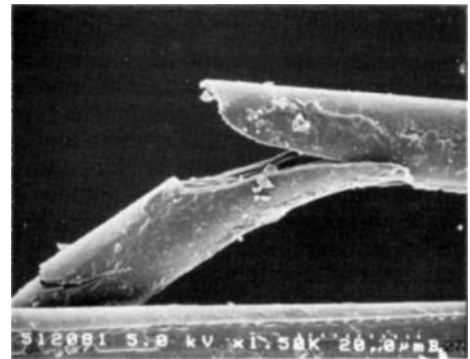
3



4



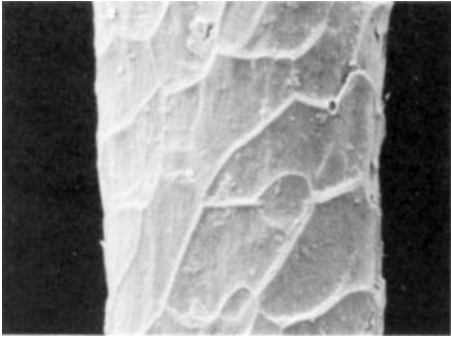
5



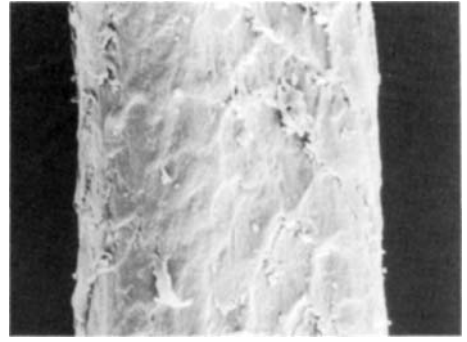
6

Plate 16G — Effects of ultra-violet exposure of polyester fibres, courtesy of D. Salem and S.B. Ruetsch, TRI, Princeton (continued).

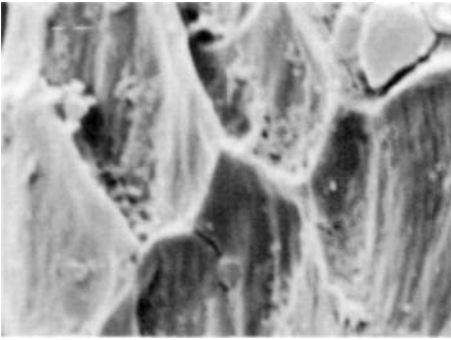
(1) Step fracture of textile molecular weight fibre spun at 5500 m/min. (2),(3) Skin-core effects in textile molecular weight fibre spun at 7000 m/min. (4)–(6) Damage in heat-set textile molecular weight fibres spun at 7000 m/min. All after alternating UV exposure and humidification.



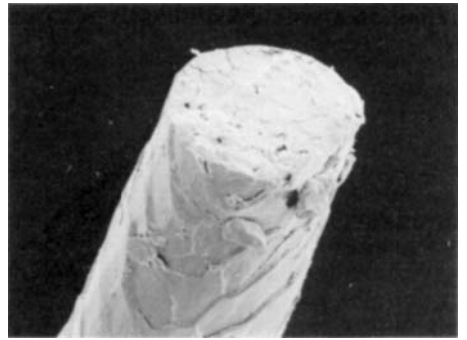
1



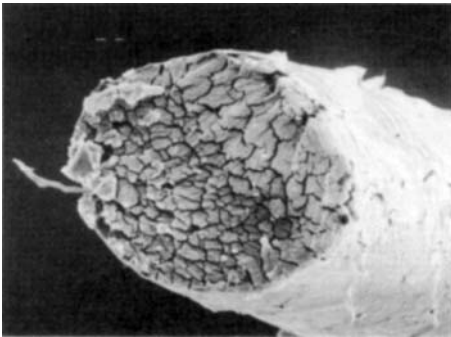
2



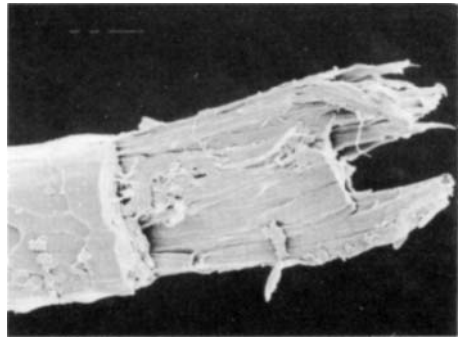
3



4



5



6

Plate 16H — Effect of ultra-violet exposure on wool, from Diane Jones, UMIST

(1) Surface of unexposed wool. (2),(3) Surface of UV-exposed wool. (4) Tensile break of unexposed wool. (5),(6) Tensile breaks of UV-exposed wool.

17

TWIST BREAKS

Although the overwhelming majority of laboratory fibre breakage tests are carried out by axial extension to the breaking point, it is also possible to twist fibres until they break. In many cases, the essential failure mechanisms are the same, although the geometry of the rupture is changed by the different direction of deformation. For example, **17A(1)** shows a brittle fracture in a glass fibre, with cracks following the line of twist.

In nylon, twist breaks usually show a ductile V-notch, angled to the fibre axis in the twist direction, followed by a catastrophic region, **17A(2)**, but the fibre can also split in two, **17A(3),(4)**.

In addition to simple twisting to break, fibres can be cyclically twisted alternately in either direction and fail by torsional fatigue. In nylon, this leads to coarse multiple splitting, **17A(5),(6)**. Other studies of torsional fatigue have been reported by Van der Vegt (1962) and Goswami, Duckett and Vigo (1980).

The twist breaks of acrylic fibres range from simple twist distortions of the granular fracture, **17B(1),(2)**, influenced also by the dog-bone cross-section of Orlon, through some degree of splitting, **17B(3)**, to breaks in which splitting is a predominant effect, **17B(4)–(6)**.

Twist breaks of rayon fibre also show a typical granular break, **17C(1)**, and the occurrence of transverse cracks, **17C(2)**, similar to those found in tensile breaks, suggests that the tension generated by the prevention of contraction on twisting is an important factor. The acetate twist breaks, **17C(3),(4)**, show similar effects.

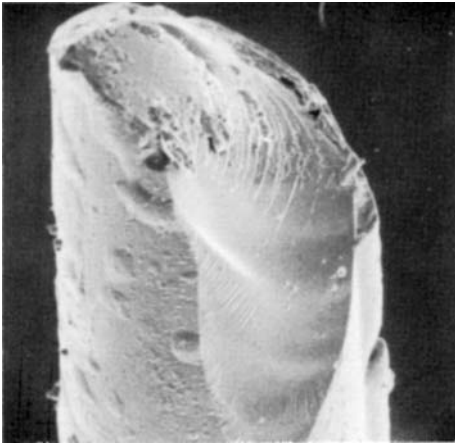
In the high-strength, para-aramid fibre, Kevlar, twisting at constant length generates tensile stress, and the rupture comes from axial splitting, **17C(5)**; but if the twisting is carried out at a constant small tension, much higher twist levels can be reached and the fibre is more sharply ruptured, **17C(6)**.

The most extensive studies of torsional fatigue have been made at the University of Tennessee. Using a single station tester, Goswami *et al* (1980) investigated the torsional fatigue of a medium-tenacity commercial polyester fibre. The applied tension of about 0.1 mN/dtex, which is about 0.2% of break load, was low. At the high torsional strain amplitude of about 10°, failure occurred in about 500 cycles and the breaks were similar to the twist breaks of nylon fibres in **17A**. However, at a lower strain amplitude, about 3°, failure took about 6000 cycles and the breaks were different. **17D(1),(2)** show two ends of a fibre, which has formed a helical snarl and failed due to torsional fatigue under these conditions. Along most of the fibre there are skin-deep cracks, but near the point of break the cracks have penetrated into the core of the fibre. The damage and deformation are similar to that found in a pill extracted from a polyester/cotton shirt.

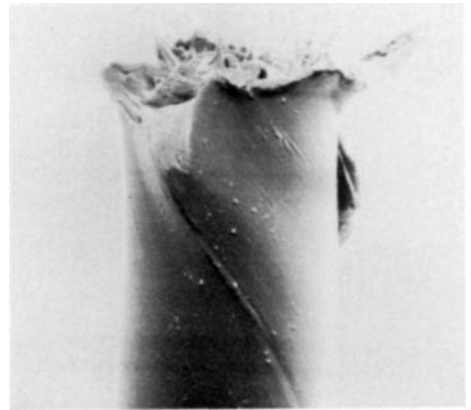
Using a multi-station tester, developed by Duckett and Goswami (1984), studies of the effect of structure of polyester fibres on torsional fatigue were carried out by Fu-Min *et al* (1985). The fibres were fairly thick and had been spun at different sizes to have almost the same diameters, about 50 µm, after drawing. When cycled with a strain amplitude of 15° under a nominal tension of 0.2 mN/dtex, a partly drawn fibre, with a draw ratio of 1.65 and a break extension of 157%, showed no loss of strength up to 1000 cycles. It then rapidly lost 70% of its strength, followed by a slower drop until catastrophic failure occurred at about 25000 cycles. A highly drawn fibre, with a draw ratio of 5.08 and a break extension of 20%, had lost 10% of its strength by 1000 cycles; then a further 70% loss took place gradually to about 100000 cycles, followed by a rapid drop.

17D(3)–(6) show the progressive change during cycling of the partly drawn fibre. This

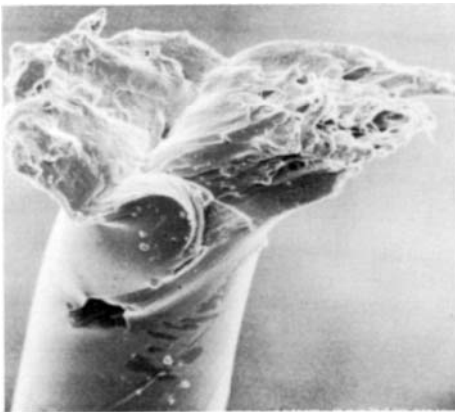
starts with transverse cracks, followed by axial cracks and finally more plastic deformation. A tensile break after cycling, **17D(7)**, shows coarse axial splitting. The damage in the highly drawn fibre at two levels of cycling is shown in **17D(8),(9)**. Tensile rupture after torsional fatigue, **17D(10)**, shows an extremely high degree of axial splitting.



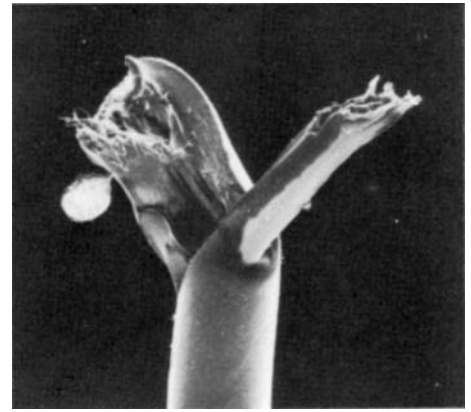
1

|—| 10 μm 

2

|—| 10 μm 

3

|—| 10 μm 

4

|—| 20 μm 

5

|—| 20 μm 

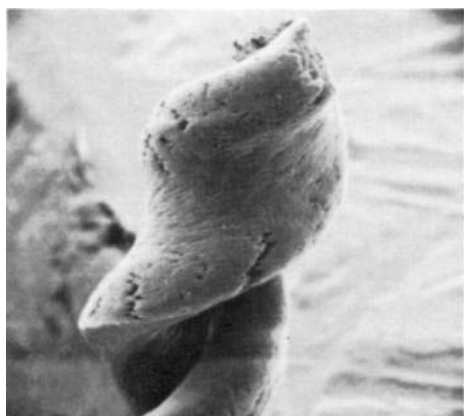
6

|—| 20 μm **Plate 17A — Twist breaks.**

(1) Glass fibre. (2-4) Nylon 66, 17 dtex, twisted to break at constant length, failing at a twist factor of about $100 \text{ tex}^2 \text{ cm}^{-1}$.

Torsional fatigue.

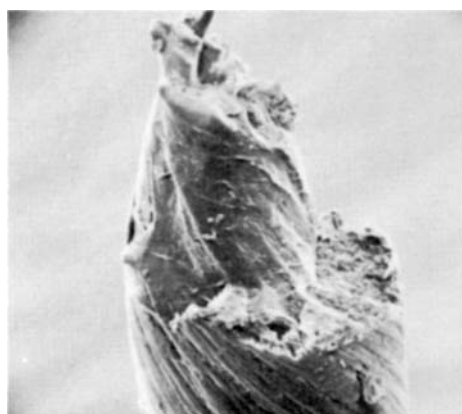
(5),(6) Nylon 66, 17 dtex, cycled to $\pm 47^\circ$ at 5.2 Hz for 13 hours.



1

|—| 20 μm 

2

|—| 10 μm 

3

|—| 10 μm 

4

|—| 20 μm 

5

|—| 20 μm 

6

|—| 10 μm

Plate 17B — Twist breaks of acrylic fibres.

(1),(2) Orlon, 17 dtex. (3),(4) Courtelle, 17 dtex. (5),(6) Acrilan, 17 dtex.

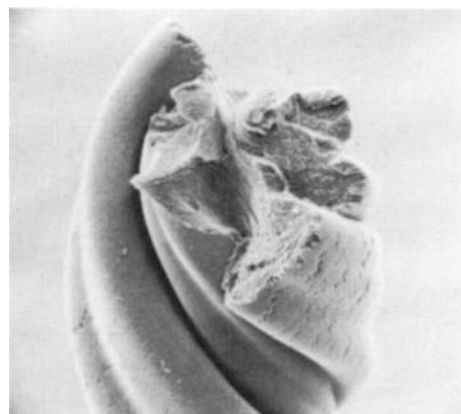
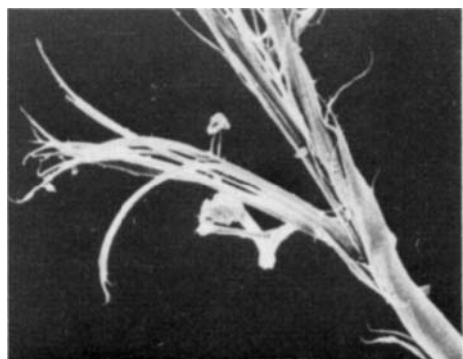
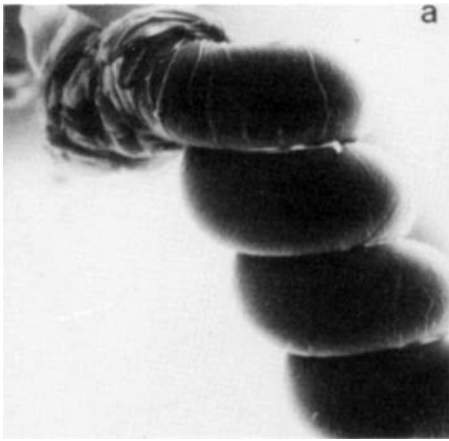
1 |—| 20 μm2 |—| 2 μm3 |—| 10 μm4 |—| 10 μm5 |—| 20 μm6 |—| 10 μm

Plate 17C — Twist breaks of cellulosic fibres.

(1),(2) Viscose rayon, Fibro, 20 dtex. (3) Secondary acetate, Dicel, 6 dtex. (4) Triacetate, Tricel, 14 dtex.

Twist breaks of para-aramid fibre (Kevlar).

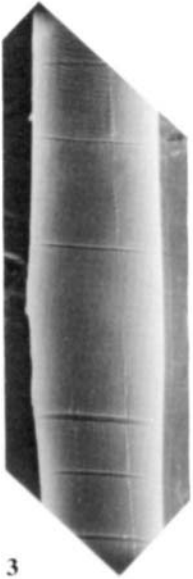
(5) Twisted to break at constant length, failed at $30 \text{ tex}^2 \text{cm}^{-1}$ (12°). (6) Twisted to break at constant tension of 27 mN/tex , failed at $73 \text{ tex}^2 \text{cm}^{-1}$ (45°).



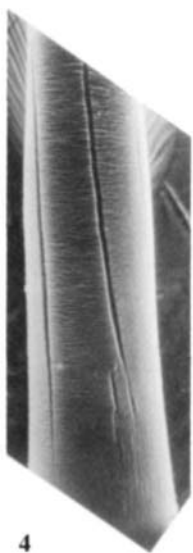
1



2



3



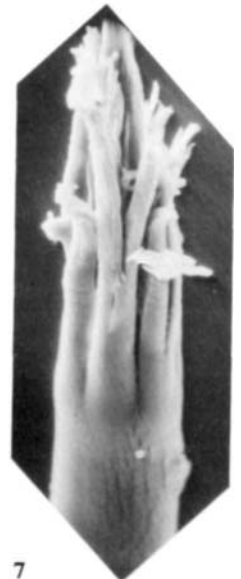
4



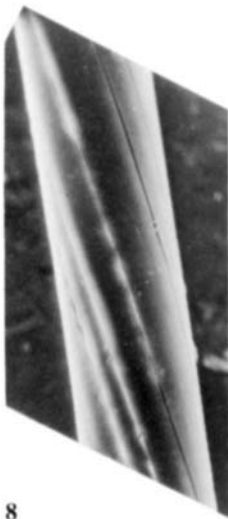
5



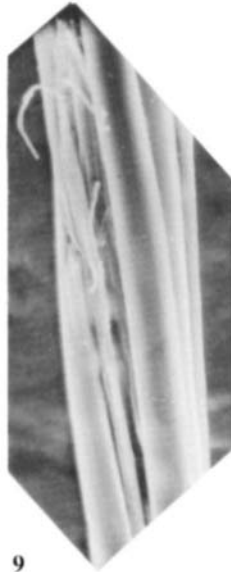
6



7



8



9



10

Plate 17D — Torsional fatigue of polyester fibres, courtesy of B.C. Goswami, Clemson University.
 (1),(2) Opposite ends of a commercial fibre, broken after torsional cycling with an amplitude of about 3° .
 (3)–(6) Progressive damage of a partly drawn fibre after cycling at 15° amplitude, 1000, 3000, 6000 and 12000 cycles. (7) Tensile break of partly drawn fibre after 3000 torsional cycles. (8),(9) Damage in a highly drawn fibre after 3000 and 15000 cycles. (10) Tensile break of highly drawn fibre after 150000 cycles.

18

COTTON

Cotton shows different forms of tensile break, depending on the environmental conditions and on any chemical modification of the fibre. The common form of rupture of cotton at 65% r.h., **18A(1)**, shows an axial split which runs round the fibre and then tears back along the fibre, as indicated schematically in Fig. 18.1. This reflects the structure of the cotton fibre, which is formed as a hollow tube of helically wound microfibrils. On drying, there is a collapse to a kidney-shape. Zone A is the most tightly packed structure and zone C is the most disturbed and internally buckled. A line of weakness runs along the fibre between zones A and C. Furthermore, at intervals the fibrils reverse direction from a left-handed to a right-handed helix. When the fibre is put under tension, the reversal point will tend to untwist in order to elongate the fibre, as shown in Fig. 18.2, and this generates shear stresses which cause the axial splitting between the fibrils. The split runs round the fibre until it reaches the line of weakness, and then tears back.

At the reversal itself, the fibrils (and the cellulose molecules) will be axially oriented, so that this is a zone of high strength. But close to the reversal the change of orientation generates additional stress concentrations, and so the break normally starts adjacent to a reversal, as in **18A(1)**.

Although the form described above is the commonest form for untreated cotton at 65% r.h., there is considerable diversity, with some breaks being shorter, **18A(2)**, and others longer **18A(3)**. Similar forms of break are found in mercerized cotton **18A(4)** at 65% r.h.

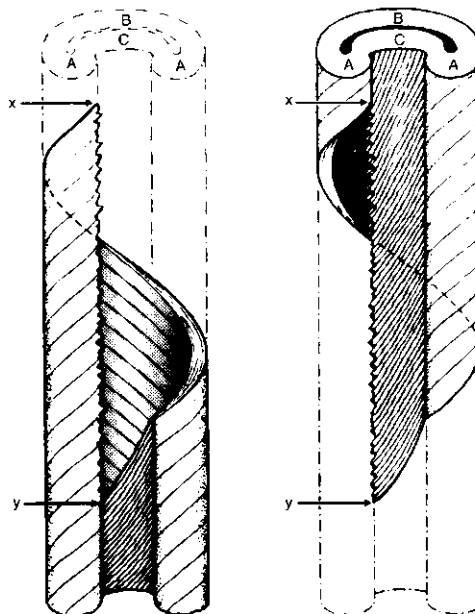


Fig. 18.1 — Typical, but somewhat idealized, form of break of cotton fibre. The full lines show the two opposite broken ends, with the dotted lines being the 'missing parts'. The break starts at x and runs as a crack along the spiral angle through zones A-B-A-C to y on the AC boundary on which it started. It then tears, somewhat irregularly, along the line xy.



Fig. 18.2 — Untwisting under tension at a reversal point.

In other conditions, other forms are found. The break of untreated cotton when wet was described in Chapter 9, as a particular form of rupture, namely independent fibrillar failure.

If the cotton fibre has been chemically cross-linked by resin treatment, the cellulose fibrils hold more firmly together and axial splitting is hindered. The breaks at 65% r.h. show distorted forms of granular break across the fibre, possibly with a short length of axial separation linking different zones of transverse fracture, as in **18B(1)**. Detail of the granular breakage is seen in **18B(2)**. In other examples, such as **18B(3)**, the break, which is adjacent to a reversal, runs in a single transverse fracture round the fibre. Similar transverse breaks are found in untreated cotton at 0% r.h., when the fibrils are hydrogen-bonded together, and at 65% r.h., if a very short test length is selected with the exclusion of any reversal, so that the shear stresses due to untwisting are not present.

In wet conditions, the greater freedom allows a long split to develop in cross-linked, resin-treated cotton, **18B(4)**.

The selection of the type of break depends on the degree of chemical attraction between the fibrils, and the changes in the form of breakage may be summarized as follows:

- | | |
|---|---|
| (a) <i>strong interaction</i>
raw cotton at 0% r.h.;
cross-linked at 65% r.h. | granular break, across
fibre, characteristic
of bonded fibrillar elements |
| (b) <i>weak interaction</i>
raw cotton at 65% r.h.;
cross-linked, wet | axial split between
fibrils |
| (c) <i>very weak interaction</i>
raw cotton, wet | independent fibrillar
break |

Twist breaks of cotton show axial splitting, with a rather sharp tearing off at the end of the broken fibre, **18C(1),(2)**. The break is similar to a twist break of Kevlar, **17C(6)**.

Tensile fatigue testing of cotton leads to marked separation of fibrils before failure, **18C(3)**.

Fatigue testing of cotton by biaxial rotation over a pin is complicated by the shape of the fibre, which gives uneven movement, and by the variability of fibre diameter, which makes it difficult to standardize strain levels. The scatter of results is large, and no significance should be attached to the differences in lifetimes in the captions to **18C(4)–(9)**. Another complication is that the torque developed in the test alternately increases and decreases the natural reversing twist in the fibre, **18C(4)**. A typical raw cotton break in air shows multiple splitting, similar to that found with other fibres, **18C(5)**. After testing in water, **18C(6)**, the broken end tapers to a point, but this may be a result of the split portions being twisted together, and then bonded on drying before examination.

The chemically treated fibres also fail by multiple splitting, **18C(7)–(9)**.

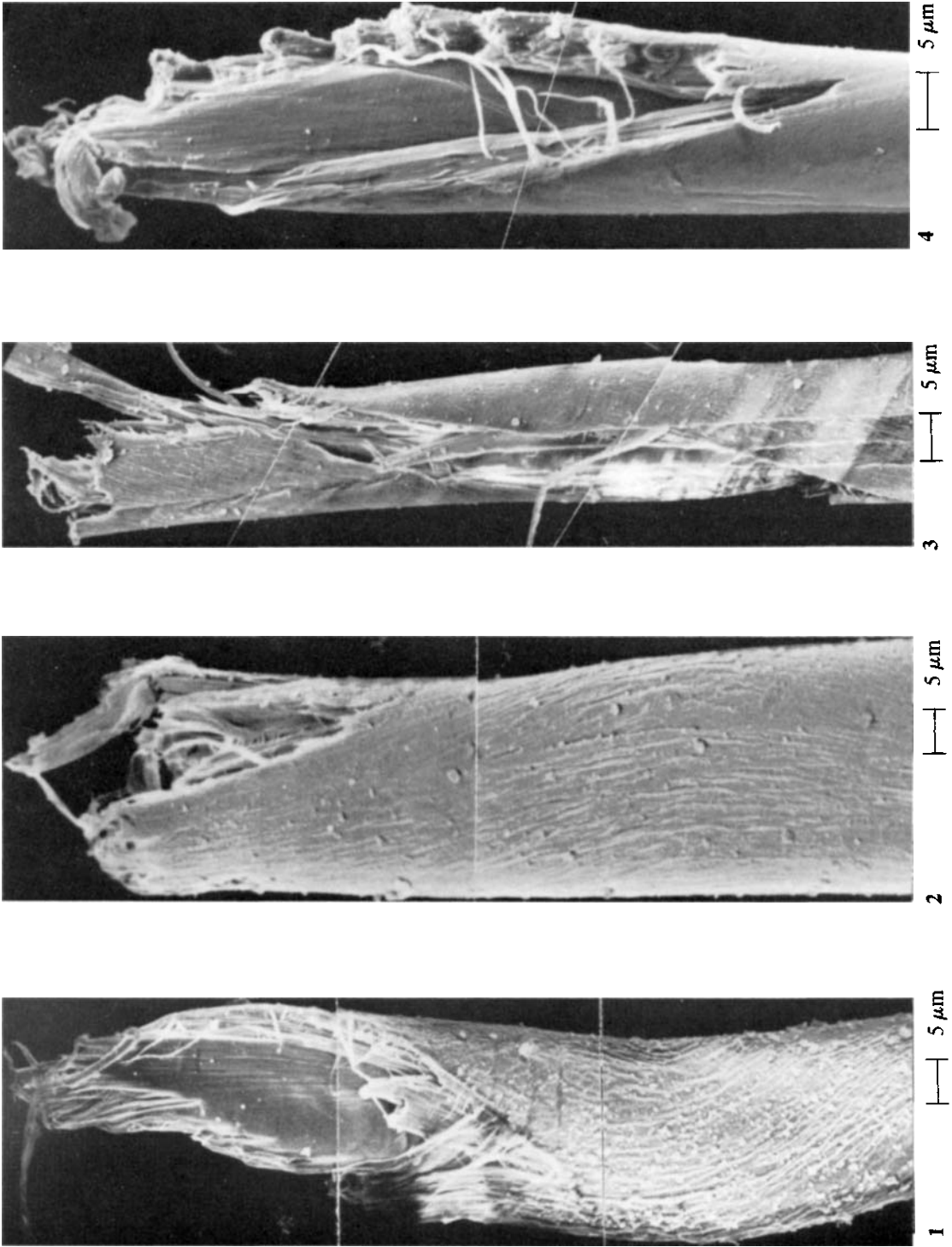
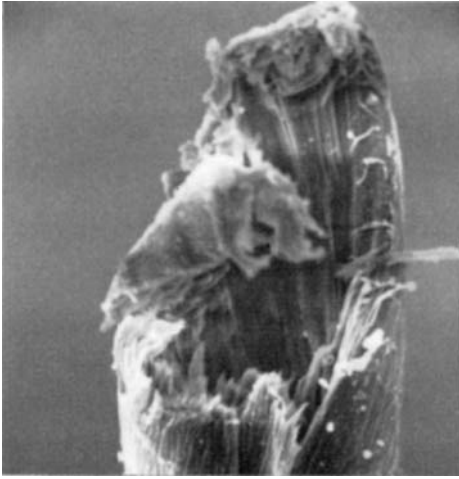
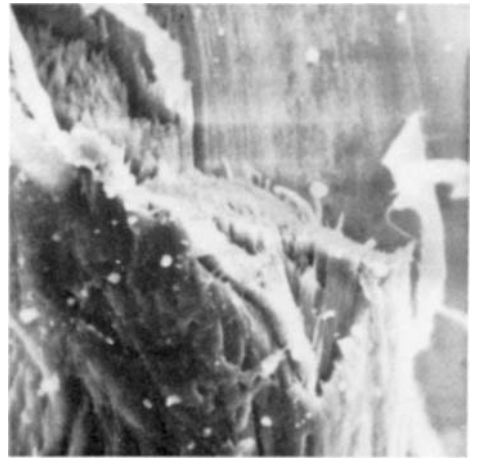


Plate 18A — Tensile breaks of cotton at 65% r.h.

(1)–(3) Raw cotton. (4) Mercerized cotton.



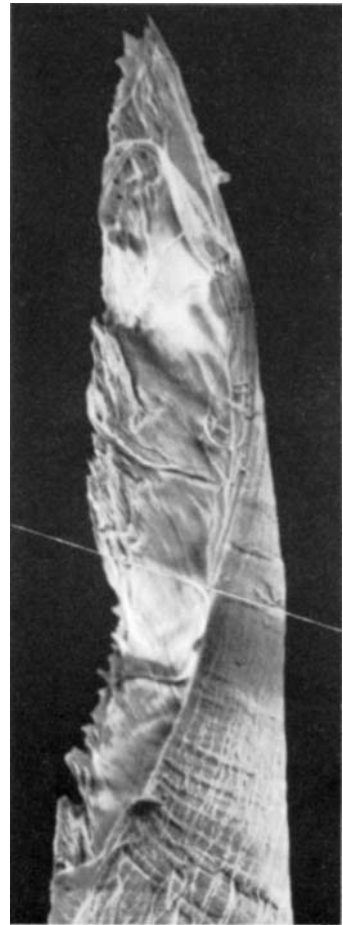
1

5 μm 

2

2 μm 

3

5 μm 

4

5 μm

Plate 18B — Tensile breaks of resin-treated (cross-linked) cotton.
 (1)–(3) At 65% r.h. (4) In water.

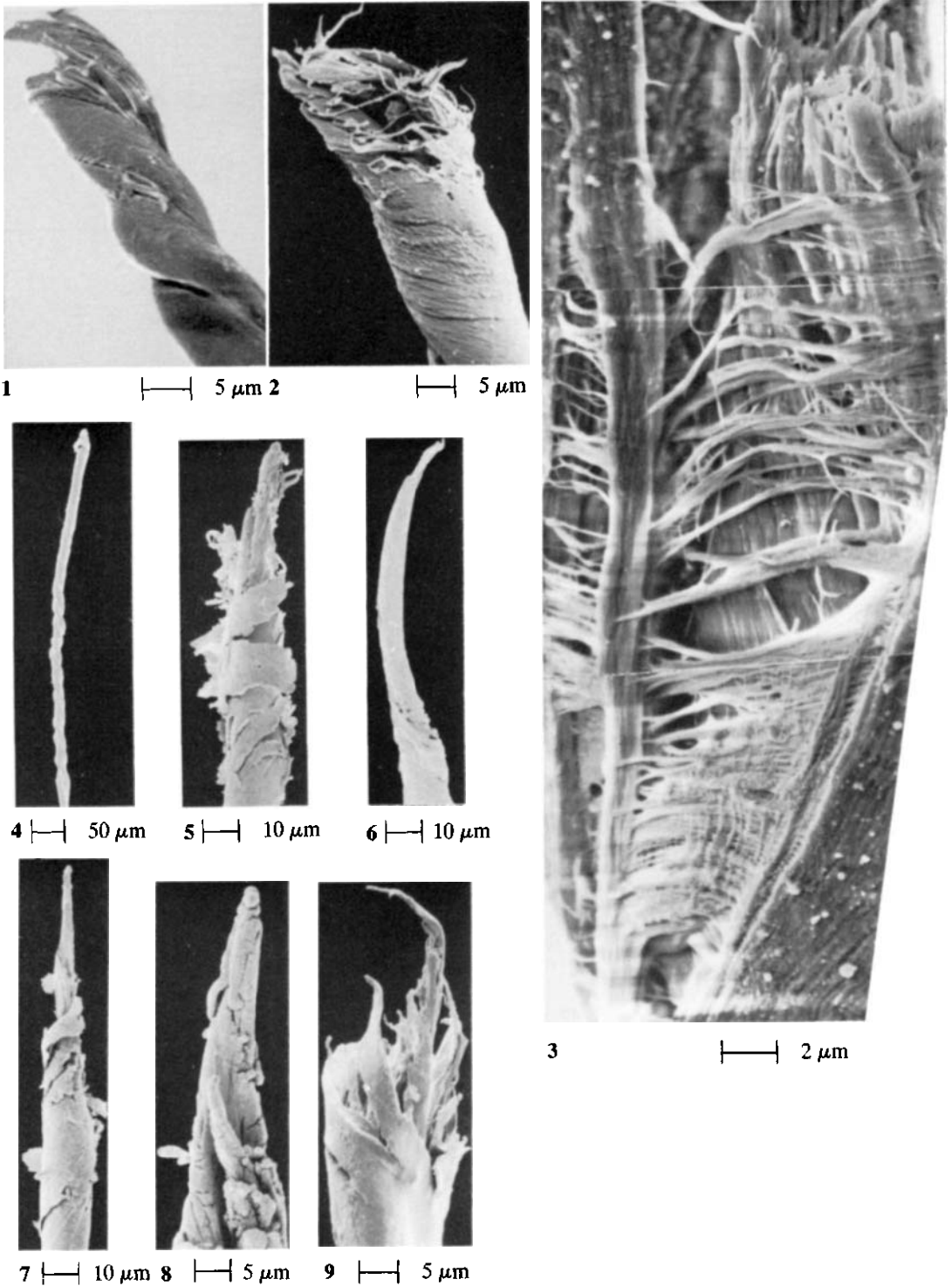


Plate 18C — Twist breaks of cotton.

(1) Raw cotton. (2) Mercerized cotton.

Tensile fatigue.

(3) Raw cotton.

Biaxial rotation fatigue.

(4) Raw cotton at 65% r.h., failed at 1898 cycles. (5) Raw cotton at 65% r.h., failed at 903 cycles. (6) Raw cotton in water, failed at 3499 cycles. (7) Prograde-treated cotton at 65% r.h., failed at 7762 cycles. (8) Mercerised cotton at 65% r.h., failed at 5979 cycles. (9) Resin-treated cotton (10% Fixapret) at 65% r.h., failed at 1334 cycles.

19

WOOL AND HUMAN HAIR

Wool and hair are natural fibres with structural features at many levels. Chemically, they are made of a mixture of complex proteins. In physical fine structure they consist of crystalline fibrils, with the molecules in helical coils, embedded in an amorphous matrix. In biological structure they are composed of separate cells, differing in composition from one part (ortho-) of the central cortex to another part (para-), and with a special form of cuticle cells or scales on the surface.

The tensile break of wool is commonly a granular fracture running across the fibre, **19A(1),(2)**, but it often splits into two separate breaks linked by an axial split, **19A(3),(4)**. It is not certain whether the central split is present before the transverse cracks appear, and thus divides the fibre into two parts, which break independently, giving the form shown in Fig. 19.1(a); or whether the transverse cracks form first, and then join up by an axial split as in Fig. 19.1(b). Both the length of the split in **19A(3)** and the continuation of the split in **19A(4)** suggest that the axial split is there first. Sometimes, there are more than two steps, **19A(5)**.

Human hair, perhaps because it suffers a greater variety of chemical and mechanical treatment, shows an even greater diversity of form than wool. The break of dry hair may be a single plane running perpendicularly across the fibre, **19B(1)**, with a granular surface similar to the breaks of solution-spun fibres in Chapter 8. However, this simple form may be complicated by steps, axial splits, separate breakage of the cuticle and fibrillation.

Most of these features can be seen in the montages of two matching ends, shown over the whole failure length in **19B(2)** and in part in **19B(3)**. The rupture is in three main steps. The break appears to start at X in **19B(3)**, and radiates from a point on the fibre surface until it reaches the first short axial step. The second transverse surface at Y reaches the major split at the centre of the fibre. This split is inclined at a small angle to the fibre axis, and thus causes a tapering over the long length (many fibre diameters) that reaches to the third transverse fracture at Z, which completes the break. Both the second and third fracture surfaces are smaller in area compared with the single planar surface near X. Two contrasting aspects of axial splitting can be seen in **19B(3)**: the central split continues for a long distance past the

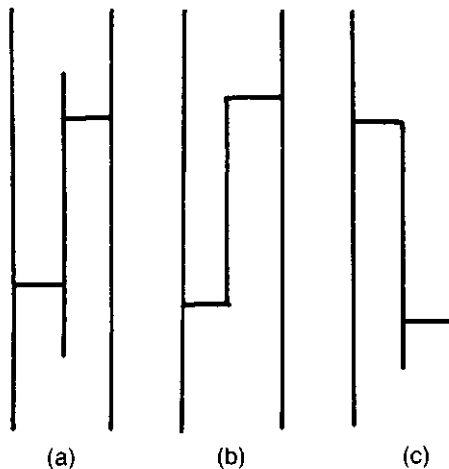


Fig. 19.1 — Three possible combinations of transverse and axial cracks.

transverse break at Y, but the other short axial split stops at the transverse fracture, X. On the other end, as seen in **19B(2)**, with corresponding locations marked X', Y', Z', the central split Y' Z' does not continue past the transverse break at Z'. Examination of breaks of many fibres suggests the occurrence of all three possible combinations, shown in Fig. 19.1, of splits stopping or continuing.

It must be emphasized that the suggestion that the break starts at X is speculative. It is possible, but unlikely, that the break starts at the other end, Z, turns into an axial split, ZY, and that a subsidiary final stage of break occurs at X and Y. Another feature visible in **19B(2),(3)**, is some short fibrillation on the surface of the axial splits.

It is difficult to know whether the complicated forms found in breaks of hair are due to the interaction between the mechanics of stress distribution and some random variations in structure or in damage within the fibre, or whether they derive from the major structural features of wool and hair fibres, namely the divisions of the cortex into two halves, with the cuticle being a third region. The break shown in **19B(4)** could easily form the basis for a schematic drawing of the fibre structure, with the central split dividing the ortho-cortex from the para-cortex, and the scale cells of the cuticle clearly seen at the edge. However, study of the other end of the break, **19B(5)**, does make clear that the sharp fracture of the scales also includes a portion of the cortex. Another feature clearly seen in **19B(5)** is a plug of material, somewhat out of focus, which runs down the length of the axial split and extends for some distance into the other end. Re-examination of **19B(4)** shows where this plug fits.

Examples of variant forms of splits and plugs in broken dry hair fibres are shown in **19C(1),(2)**.

Breaks of wet hair, **19C(3)–(5)**, are usually similar to breaks of dry hair. However, the fibrillation is often more pronounced, with longer strips of material pulled away from fracture surfaces. An extreme example is shown in **19C(6)**.

Tensile fatigue of wool and hair intensifies the tendency to axial splitting, and very long breaks are common, **19D(1)**. In one example of fatigue failure in human hair, the break had the stake-and-socket form, **19D(2)–(4)**, which is illustrated in **16D(1),(2)** and is type 7 in Fig. 1.5. In this situation it could be regarded as a variant of the form of tensile fatigue failure found in nylon and illustrated in Fig. 11.2, except that the initiating transverse crack encircled the fibre and caused the axial split to run conically into the centre of the fibre. The tendency of wool and hair to develop axial splits under oscillating tensile stress may well be a cause of split fibre ends, which can be a problem in human hair.

Biaxial rotation fatigue of human hair in air leads to the usual mode of failure by multiple splitting, **19D(5)**. Some earlier studies, using the method of rotation over a pin with the drive from one end, showed similar breaks with multiple splits in air, and sometimes in water. Other tests in water gave a sharper form of splitting, together with some surface damage, as shown in **19D(6)**.

Typical multiple split breaks result from biaxial rotation fatigue tests of wool, **19E**. Two pairs of broken ends, **19E(1)–(4)**, show the splitting occurring over the whole break zone, with the twist in opposite directions on the two ends, due to the drag resulting from friction on the pin, and internal hysteresis. Some of the splits in **19E(1)**, and to a lesser extent in **19E(3)**, appear to be axial rather than helical, but this may be due to elastic recovery after rupture. It is also possible that the selection of lines of splitting is influenced by the multicellular morphology of wool fibres. In the third pair, **19E(5),(6)**, there are two zones of splitting, similar to the polyester fibre in **13C(7),(8)**, with considerable surface wear in the region between zones caused by rubbing on the pin. The effects are thus similar to those discussed in Chapter 13. There is very high statistical variability in the test results on wool fibres, due to variability in diameter, which influences the level of strain in bending, and in structure or selective damage.

Flex fatigue of wool by pulling backwards and forwards over a pin can lead to both surface wear and axial splitting, **19F(1)**, which are two of the forms discussed in Chapter 12. In some tests, **19F(2)**, surface wear was dominant, with the final failure being a tensile break over a reduced cross-section, similar to effects in surface wear from a rotating pin, as was shown in **14A(4)**. In other samples, **19F(3),(4)**, the multiple splitting was dominant.

Similar tests on human hair also showed clear evidence of surface wear, **19F(5)**; but there were also very complicated final breaks, **19F(6)**, reflecting a strong influence of the cellular structure of hair.

Another form of damage, which occurs in wool, results from attack by the larvae of moths and beetles, which are able to digest cross-linked proteins as a source of food. A bite mark of the larva of the furniture carpet beetle, *Anthrenus flavipes* var. *seminiveus* Casey, on wool is shown in **19G(1)**. Other examples of insect damage are given by Anderson and Hoskinson (1970) and by Cooke (1989).

An extensive investigation of larval excreta, in order to show how the breakdown of the keratinous material occurs in wool pests, has been reported by Hammers, Arns and Zahn (1987). Generally, the excreta are a mass of small granules of the same colour as the wool fabric fed to the larvae, but some fragments at various stages of digestion are found. Initially, the cuticle swells and the cells begin to lift off the cortex, as seen in the fibre in **19G(2)**, excreted by a larva of the webbing clothes moth, *Tineola bisselliella*. More severe breakdown, with partially digested cortex, fragments of cortical cells, and cortical and membrane fragments,

are shown in **19G(3),(4)**, from *Anthrenus* Casey. A collection of fibrous fragments occurs in the excreta of the black carpet beetle, *Attagenus piceus*, **19G(5)**. All the above examples are from larvae fed on untreated wool. The excreta of larvae fed only on wool treated with a low concentration of a moth-proofing agent showed similar forms of breakdown: undigested and partly digested treated fibres from *Anthrenus* Le Conte can be seen in **19G(6)**.

Studies of human hair made during the first decade of commercial scanning electron microscopy were described in a paper by Brown and Swift (1975). Referring to studies of mechanical properties and of the appearance of deformed fibres, they say:

A logical development is to combine these two techniques so that both physical and structural data could be collected simultaneously, thereby enabling a more detailed and accurate assessment of the breakdown of structural components to be made. The SEM, because of its great depth of focus, wide range of magnification and large area for specimen manipulation, has been adapted for conducting dynamic experiments in situ. In addition, the manner in which the visual information was processed made direct recording of the results on to videotape possible.

Unfortunately, stills from video-recordings do not give a good impression of the insights to be obtained by watching the moving pictures. However **19H(1)–(4)** illustrate the studies made by Swift over a number of years. The paper mentioned above includes studies made on the hair of six young women. Samples of hair, over 50 cm long, which fell out naturally with intact roots during brushing and combing, were collected, and 4 cm portions from root to tip were broken in an Instron tester. Brown and Swift (1975) noted five main types of fracture. Type 1 at the root end (similar to **19B(1)** and to **19H(5)** from the TRI studies in the next section) was 'a clean transverse fracture . . . almost as if cut with a knife . . . the cuticle has split circumferentially about the transverse fracture through the cortex'. Type 2, also near the root and similar to **19B(4)** and **19I(1)**, had 'the cortex stepped and with some disturbance of the cuticle behind the point of fracture, either in the form of a longitudinal split back from the main fracture or a narrow circumferential split some distance from the point of primary fracture.' In type 3, similar to **19C(1),(2)**, 'part of the primary fracture is transverse but the remainder tails off with segments of cortex pulled out.' In types 4 and 5, occurring near the end of weathered hair, the fracture becomes 'ragged with the cortex splitting into fibrillar elements.' This is beginning to be seen in **19C(2)**, and is clear in the extreme example of type 5, **19H(1)**. In going from root to tip, the stepped and fibrillated forms are reached more quickly for badly weathered hair, and the most extreme forms are not found in hair which has not been much weathered.

In addition to changes in the fracture of the cortex, effects are also seen in the cuticle, with some cracking and lifting of scales. A particularly severe example of scale lifting is shown in **19H(2)**. This is a picture of a human hair that had been stretched 20% in water and then steam set. The delamination and circumferential fracture of the cuticle, which results from the differences in extensibility of cortex and cuticle, have exposed the surface of the cortex.

A classic split end is shown in **19H(3)** in woman's hair, 35 cm long. The subject used no toiletry treatments except for twice-weekly shampooing, and brushing and combing about twice per day. Another hair, **19H(4)**, from the same person shows *trichorrhexis nodosa*, which is an intense focal splitting of the hair shaft revealing cortical fragments. This damage is visible as a bright node. The hair is intact on either side of the node and a droop at this point of weakness is particularly apparent with long hair styles. The problem is found with people who spend excessive amounts of time in the sun, since the mechanism is embrittlement due to crosslinking of the plasticising components of the hair by free radicals induced by ultra-violet exposure.

RESEARCH ON HUMAN HAIR AT TRI PRINCETON

by H-D. Weigmann and S. B. Ruetsch

Keratin fibres have a rather complex cellular morphology consisting basically of an assembly of closely packed cortical cells, which are surrounded by single or multiple layers of cuticular cells. In human hair these can amount to up to ten layers at the root end of the fibre. Since grooming, weathering and cosmetic treatments impact on the cuticle, progressively fewer cuticle cells are found along the hair shaft towards the tip of the fibre. Total ablation of the cuticle cells in very long and heavily stressed fibres leads to the phenomenon of split ends, where the cortical cells lose cohesion, separate and sometimes fibrillate on a macrofibrillar level. Each of the morphological components contains various structural elements which affect its tensile, torsional, bending and shear properties. Intercellular adhesion is provided by the so-called cell membrane complex. In some hair fibres, especially those of large diameter, a loosely packed porous region called medulla is located near the centre of the fibre. In view of the complex morphology of hair fibres, it is not surprising that their fracture behaviour yields a number of interesting patterns, which sometimes permit conclusions to be made regarding the cause of damage experienced by the hair.

The application of tensile stresses results in a variety of fracture patterns, depending on molecular cohesion within the fibre. Smooth radial fractures occur most frequently when the fibre is wet and the fully swollen cortical cells press against the cuticular envelope. Initiation of fracture occurs almost exclusively at a point between cuticle and cortex — possibly at a pre-existing flaw. Only in very dry conditions have we observed crack initiation in the centre of the cortex. From its initiation, the crack propagates radially until it reaches critical size and catastrophic failure occurs, **19H(5)**. While there is obviously some unevenness in the catastrophic region of the fracture surface cortex, it appears that the cuticle fails as a unit, **19H(6)**.

A wide variety of step fractures is the most common type of fracture pattern, which reflects the presence of weak points in the intercellular cohesion within the cortex. Step fractures are most frequently observed during fracture under ambient conditions, namely 65% relative humidity. The fracture always starts as a smooth radial crack, which suddenly changes direction when it encounters a region of weak intercellular adhesion. The crack travels axially along cortical cell boundaries until it encounters another radial crack and the fibre fails. The step length can be much longer than that shown in **19I(1)**, can be angled relative to the fibre axis, and can end in a smooth, jagged or fibrillated end.

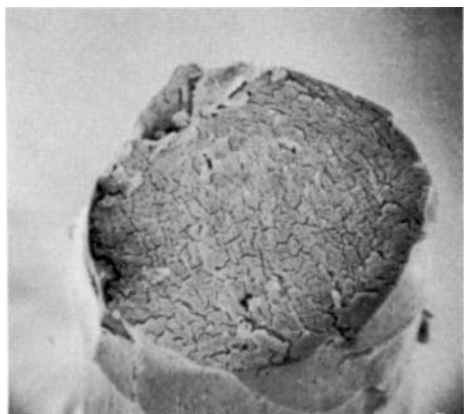
Chemical treatments such as bleaching (6% alkaline hydrogen peroxide) affect intercellular cohesion in the cortex as well as in the cuticle. This can manifest itself in long step fractures as shown in **19I(2)**, which also shows poor adhesion between cortex and cuticle resulting in a hollow cuticular sheath. This lack of adhesion is more clearly seen at higher magnification in **19I(3)**, where a loose, undulating cuticle is observed. **19I(4)** shows that failure in the cuticle also occurs in a stepwise manner with the individual cuticle cell failure, reflecting poor intercuticular adhesion.

Tensile fatigue, 100 000 cycle at 1 Hz at stresses below the yield point of the fibres, causes considerable damage to intercellular cohesion both in the cortex and the cuticle. An abundance of scale lifting is observed in the cuticle, **19I(5)**, while failure along the cortical cells shows fibrillation on the macro fibrillar level with possibly some fragments of intercellular cement also sticking out of the cell surfaces, **19I(6)**.

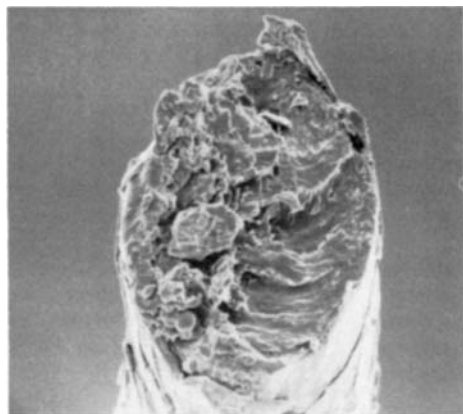
Exposure of human hair fibres to 700 hours of alternating cycles of ultra-violet radiation and humidification at 95% relative humidity results in modification gradients within the fibres, which lead to rather interesting fracture patterns, **19J(1),(2)**. High levels of photo-oxidation occur in the fibre periphery with a steep gradient to lower levels in the interior. The highly photo-oxidised, fused periphery, which includes the cuticle and outer cortical cells, has become brittle and rigid, losing its elastic properties and failing as a unit all around the fibre during extension. It would appear that radical reactions result in these outer domains. Failure in the not yet fused interior occurs in the form of a 'cathedral spire' fracture pattern (referred to elsewhere as 'stake-and-socket') at individual sites alternatively along the cortical cell boundaries and across the cortical cells tapering off to the least modified centre of the fibre. The corresponding opposite site of the cathedral spire is a hollow opening.

A shorter exposure of the hair fibres to only three hours of ultra-violet radiation and humidification preferentially results in smooth, radial fractures. The photo-oxidised periphery of the fibre has lost its original extensibility and develops deep radial cracks, **19J(3)**. As stresses increase during fibre extension, fracture is initiated between cortex and cuticle on the side opposite to the radial cracks and propagates from there in the form of a smooth fracture surface until catastrophic failure occurs, **19J(4)**.

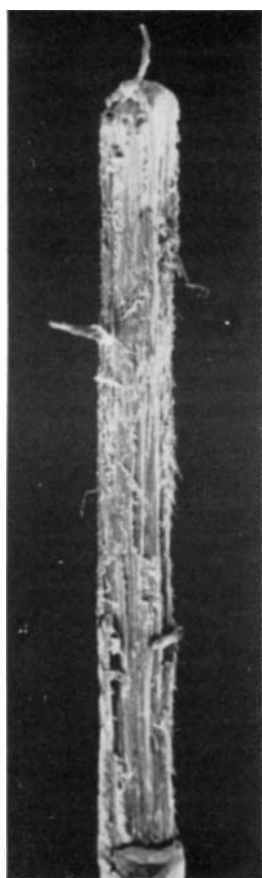
As pointed out above, the medulla seen in certain higher diameter fibres consists of an array of empty cells, which can constitute a significant part of the centre of the fibre. While the medulla does not contribute in terms of mechanical performance of the fibre, it does appear to have significant effect on the optical or light scattering of the fibres. Fibrous elements in the differentiated medullar cells apparently fuse with the cell membranes. These reinforced cell membranes cannot collapse during desiccation and thus form large intracellular cavities, which are rather stiff. During tensile failure, these medullar cells tear apart and form part of the fracture surface of the fibre, **19J(5),(6)**.



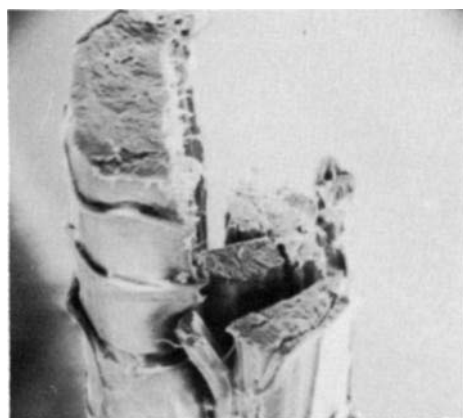
1

|—| 5 μ m

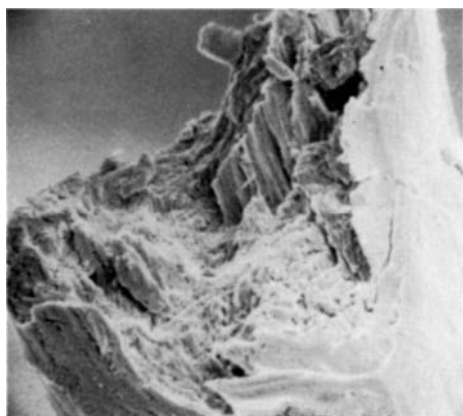
2

|—| 5 μ m

3

|—| 20 μ m

4

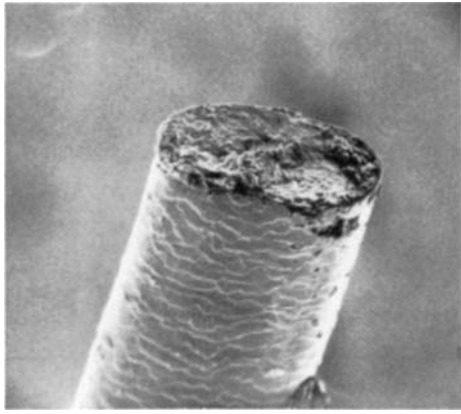
|—| 5 μ m

5

|—| 5 μ m

Plate 19A — Tensile breaks of wool.

(1) Untreated wool, 64s. (2) Untreated wool, 56s. (3)–(5) Untreated wool, 64s.



1

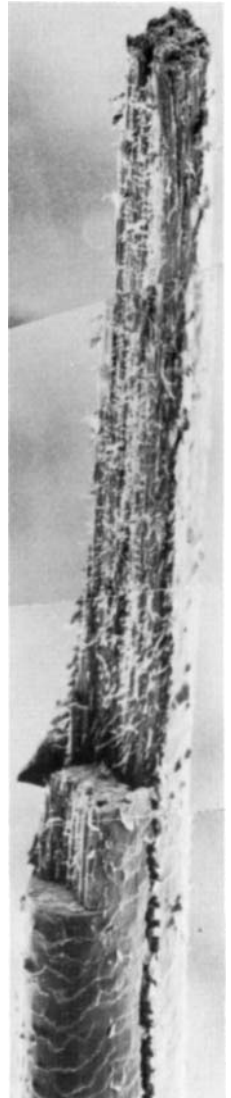
 20 μm

X'



Y'

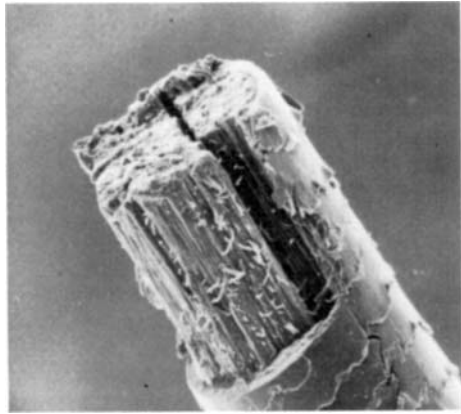
Z



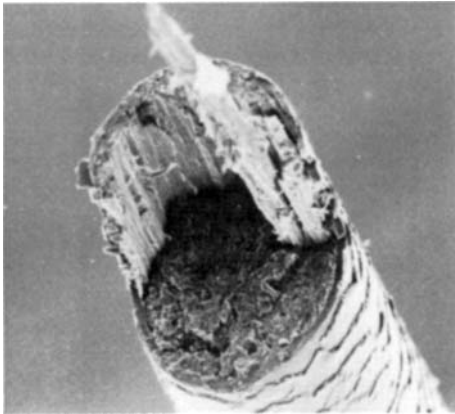
Y

X

Z'



4

 10 μm


5

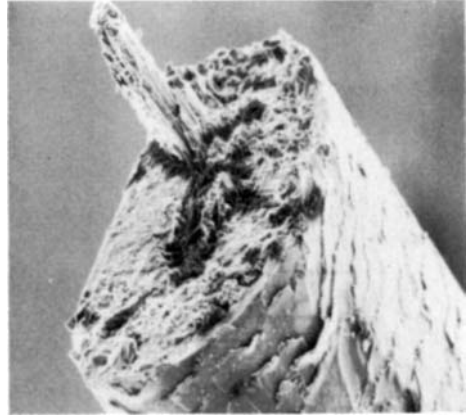
 10 μm
2 20 μm 3 20 μm

Plate 19B — Tensile breaks of dry human hair.

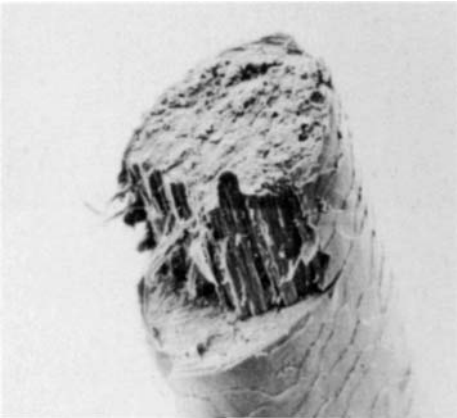
(1) Simplest form, from female subject A. (2), (3) Opposite ends of another break, showing complex features, from subject A. (4), (5) Opposite ends of break, from another female subject B.



1

30 μm 

2

10 μm 

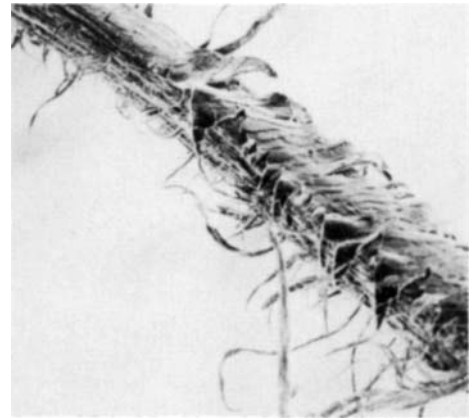
3

10 μm 

4

20 μm 

5

20 μm 

6

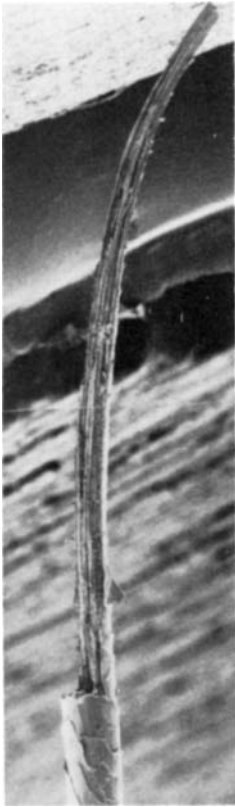
20 μm

Plate 19C — Tensile breaks of dry human hair.

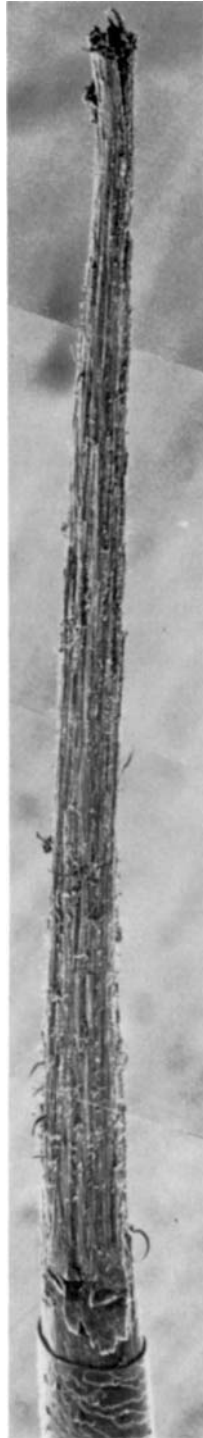
(1) From female subject A. (2) From female subject B.

Tensile breaks of wet human hair.

(3) From subject A. (4),(5) From subject B. (6) Extreme fibrillation near broken end, from subject A.



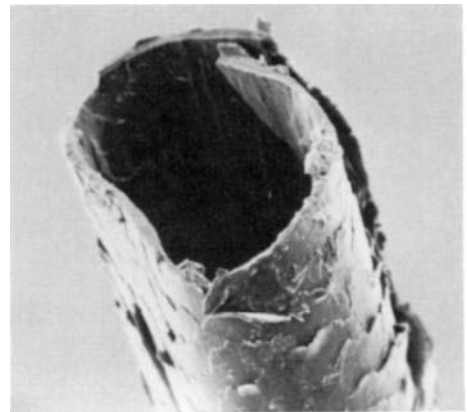
1 | 20 μm



2 | 20 μm



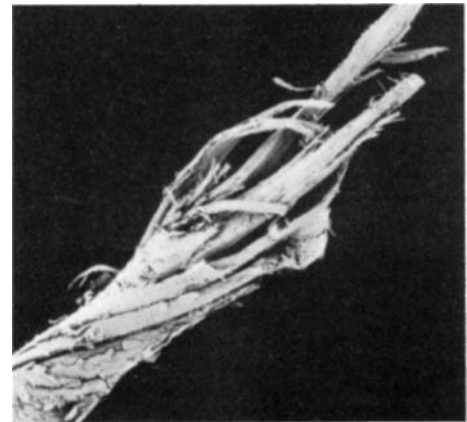
3 | 10 μm



4 | 10 μm



6 | 50 μm



5 | 50 μm

Plate 19D — Tensile fatigue breaks.

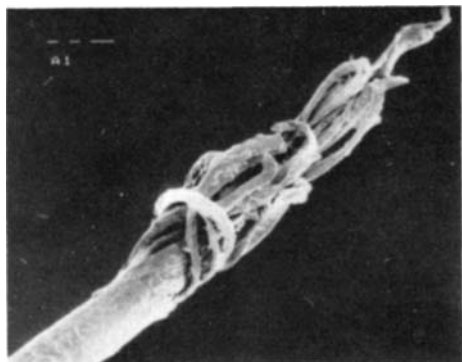
(1) 56s untreated wool. (2) Human hair. (3) Detail of break (2). (4) Opposite end of the break shown in (2), (3).

Biaxial rotation fatigue over a pin in air.

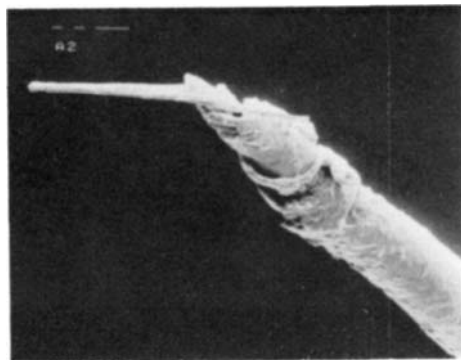
(5) Human hair.

Rotation over a pin in water.

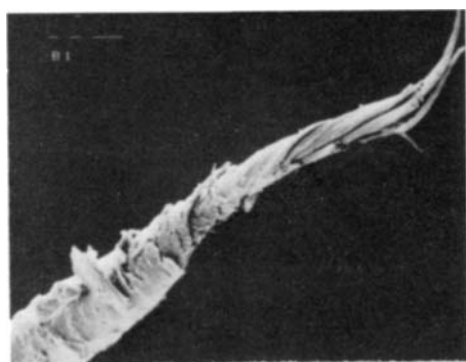
(6) Human hair.



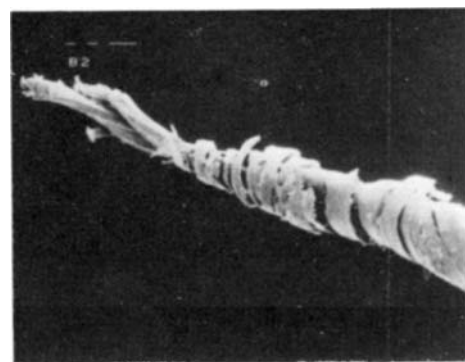
1

20 μm 

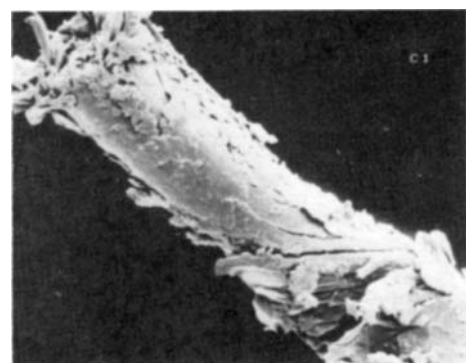
2

20 μm 

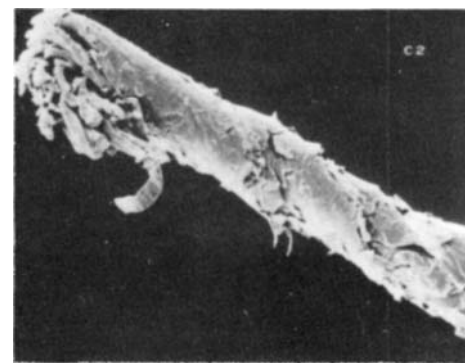
3

20 μm 

4

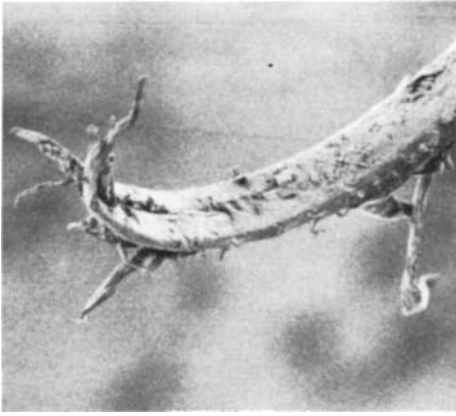
20 μm 

5

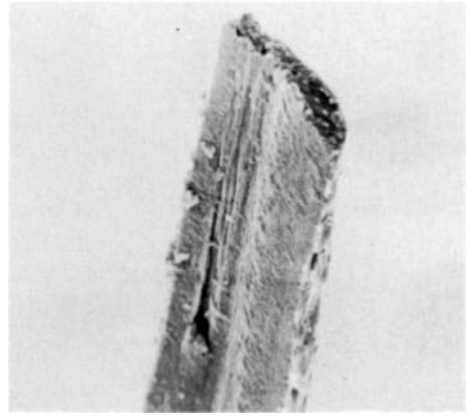


6

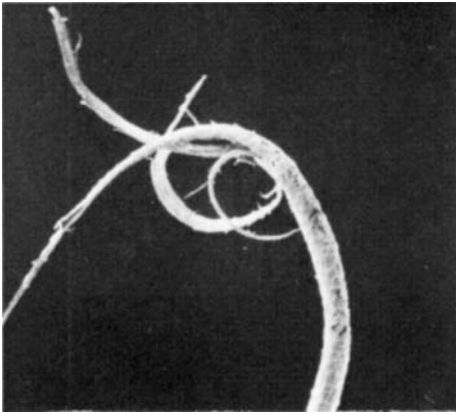
Plate 19E — Biaxial rotation fatigue of wool fibres extracted from bleached fabric tested at 120°C, 65% r.h., approximately 10% strain amplitude, and tension of about 10 mN. (1), (2) Opposite ends of fibre, which broke at 7108 cycles. (3), (4) Opposite ends of fibre, which broke at 3537 cycles. (5), (6) Opposite ends of fibre, which broke at 1550 cycles.



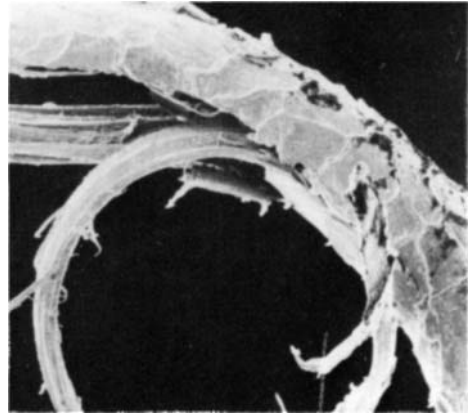
1

|—| 20 μm 

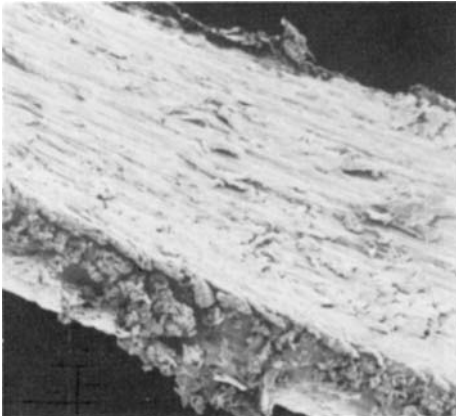
2

|—| 10 μm 

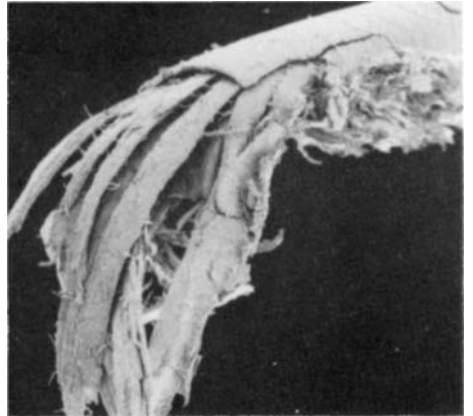
3

|—| 50 μm 

4

|—| 10 μm 

5

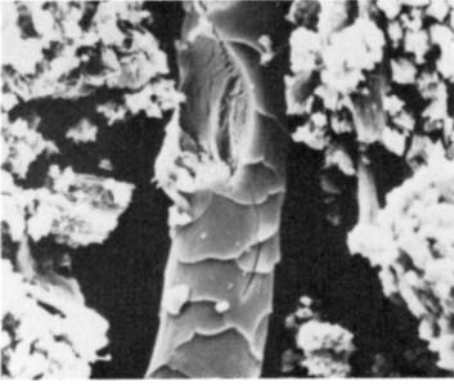
|—| 10 μm 

6

|—| 20 μm

Plate 19F — Flex fatigue by pulling to and fro over a pin.

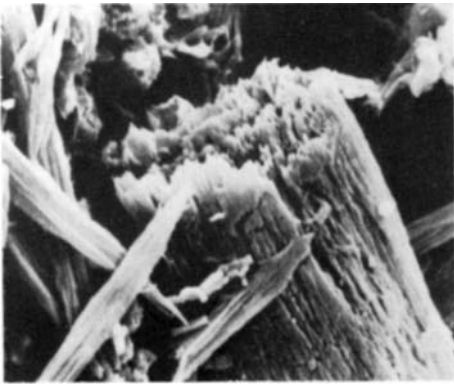
(1) Wool fibre broken after 14 750 cycles. (2) Wool fibre broken after 43 250 cycles. (3), (4) Wool fibre broken after 1 750 cycles. (5) Human hair after 5 000 cycles, before failure. (6) Human hair broken after 11 250 cycles.



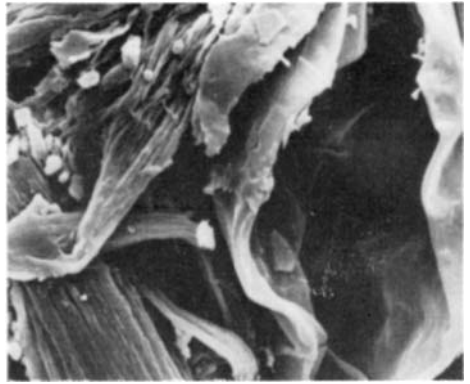
1



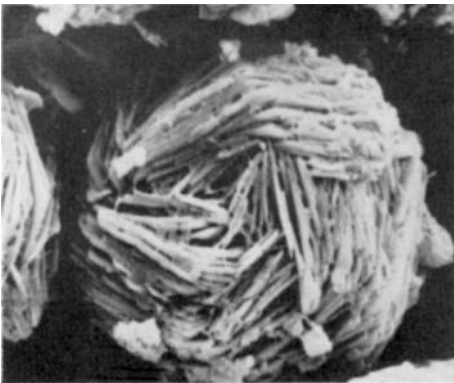
2

5 μm 

3

5 μm 

4

5 μm 

5

5 μm 

6

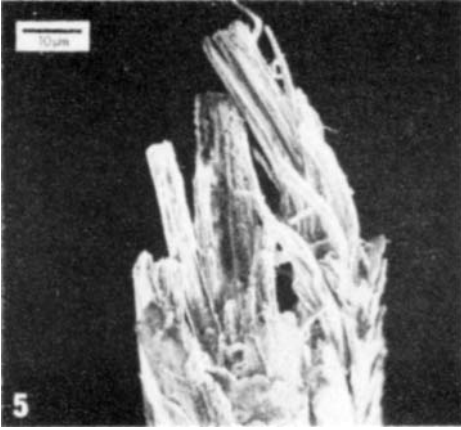
5 μm

Plate 19G — Larval bite (from I. Hammers and W. Arns, private communication).

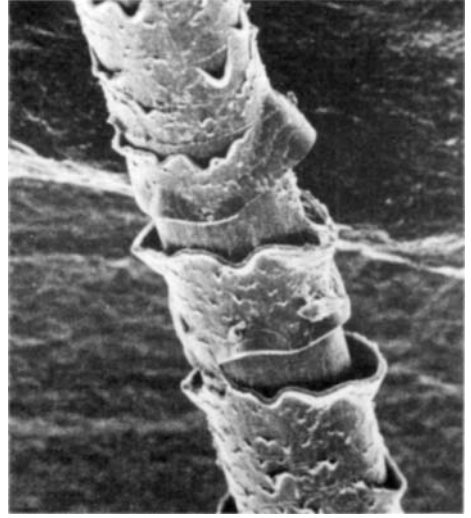
(1) Bite-mark of larva of *Anthrenus* Casey on wool fibre.

Larval excreta (from Hammers, Arns and Zahn, 1987).

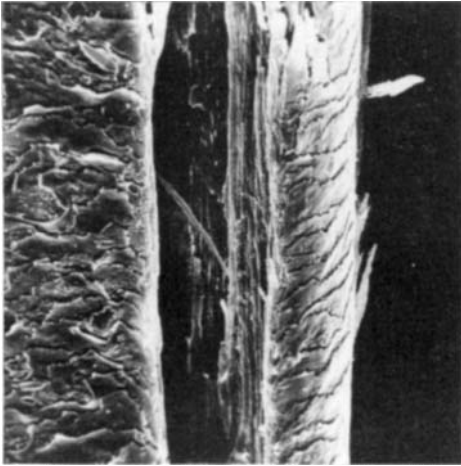
(2) *Tineola bisselliella*, fed on untreated wool. (3), (4) *Anthrenus* Casey, fed on untreated wool. (5) *Altigenus piceus*, fed on untreated wool. (6) *Anthrenus* Le Conte, fed on moth-proofed wool.



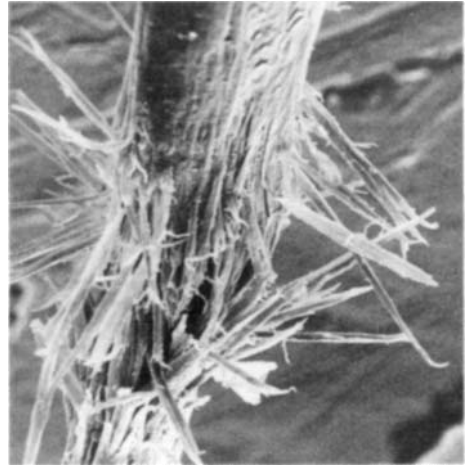
1



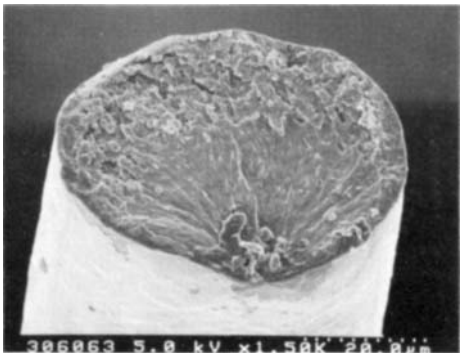
2



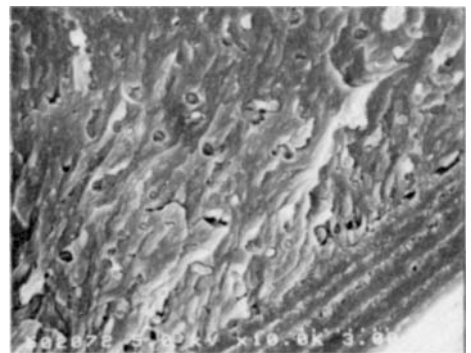
3



4



5



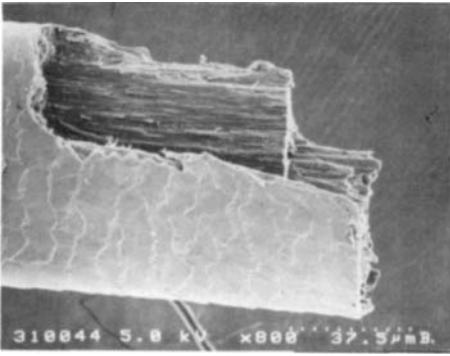
6

Plate 19H — Studies of damage in human hair by J. Alan Swift.

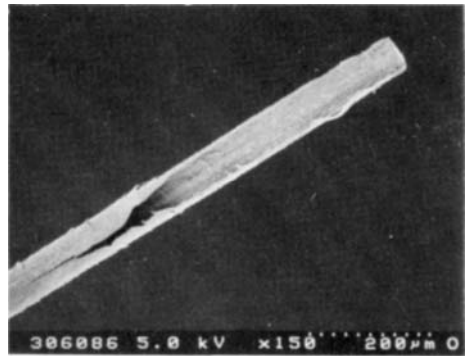
(1) Multiple splitting at the end of highly weathered hair. (2) Hair stretched in water 20% and then steam set. (3) Classic split end. (4) *Trichorrhexis nodosa*.

Studies of human hair at TRI

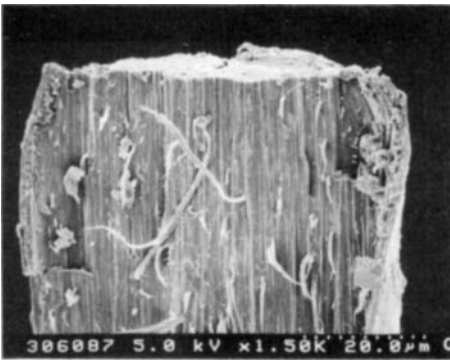
(5) A common form of smooth radial fracture of normal hair. (6) Detail near the cortex/cuticle boundary.



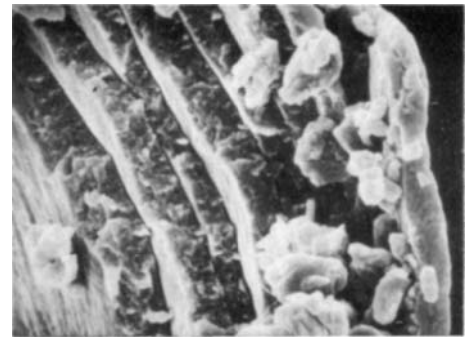
1



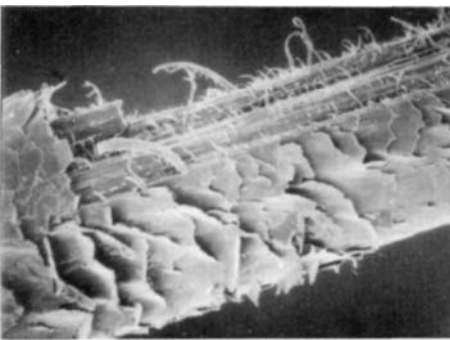
2



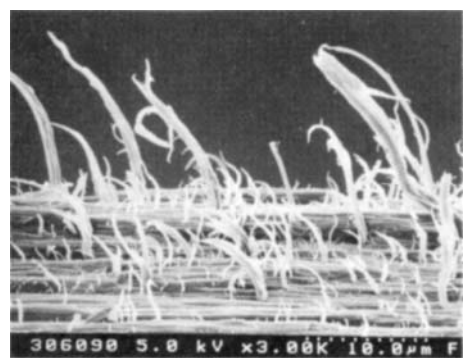
3



4



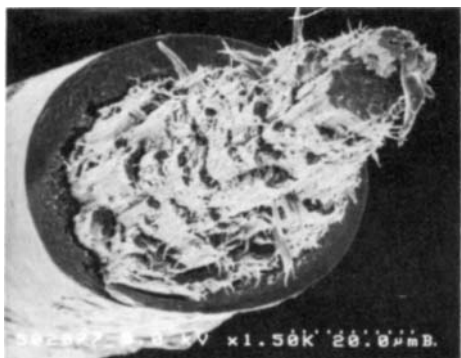
5



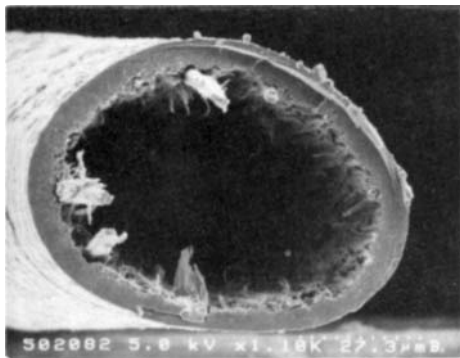
6

Plate 191 — Studies of human hair at TRI (continued).

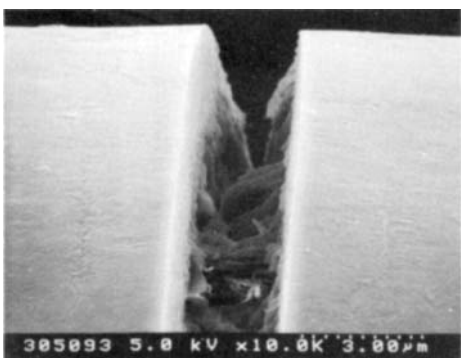
(1) Stepped tensile fracture of normal hair. (2) Long stepped fracture of hair bleached with 6% alkaline hydrogen peroxide. (3) Detail of split surface. (4) Poor intercellular cohesion in cuticle and between cortex. (5) Tensile failure of hair after 100000 cycles of fatigue. (6) Detail of fibrillation of cortical cells.



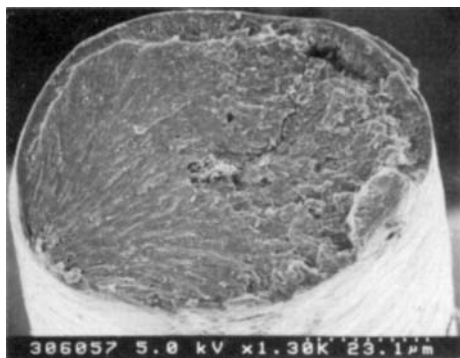
1



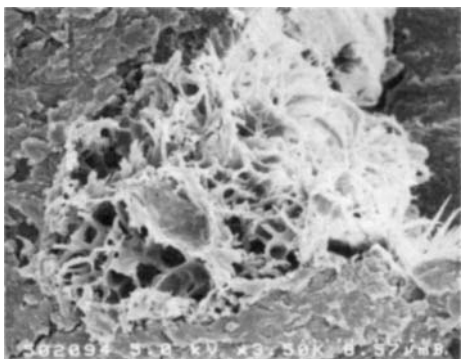
2



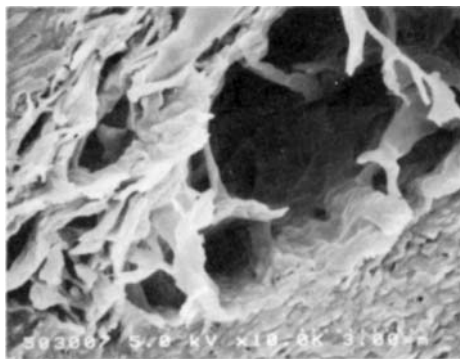
3



4



5



6

Plate 19J — Studies of human hair at TRI (continued).

(1) 'Cathedral spire' tensile fracture of hair exposed to 700 hours of alternating ultra-violet irradiation and humidification. (2) The hollow opening in the opposite end, alternatively called the socket in a 'stake-and-socket' break. (3),(4) Tensile failure of hair exposed for 300 hours of ultra-violet radiation and humidification. (5) Fracture of hair including a medulla. (6) Detail of damage in medulla.

20

OTHER FORMS OF SEVERANCE

Fibres can be severed in other ways than by the application of tensile, torsional, flexural or shear stresses. Cutting is a method which may be deliberate or accidental, and the appearance of the break depends not only on the fibre type but also on the instrument. With a blunt knife, cutting may be little more than a means of applying tension, so that the break is a distorted form of tensile failure. But with sharper instruments distinct forms occur.

A sharp razor gives a clean cut across a fibre as seen in nylon, **20A(1)**, with the only features being some grooves in the direction of cutting and a small lip at the edge of the fibre. In contrast to this, cutting with a knife shows more spreading of the break, **20A(2)**. There is some similarity to the high-speed breaks shown in Chapter 6, and a common feature may be heating of the fibre, which could occur as the knife is drawn across it.

The grooves in the end of a nylon fibre cut with a razor can be quite deep, **20A(3)**, and show interesting surface detail at high magnification, **20A(4)**. In polyester, perhaps because there is a higher resistance to cutting, there is more distortion of the fibre end in a razor cut, **20A(5)**.

Scissor cuts of nylon or polyester show a characteristic form, which is caused by the two blades pressing together, **20A(6)**.

The effects of different forms of cutting on most other fibres are broadly similar in form. A razor cut of cotton is clean, with a few grooves on the surface, **20B(1)**, and perhaps some tearing, **20B(2)**. Tearing and squashing are much more apparent in a knife cut, **20B(3)**: melting does not occur, because cotton chars before it melts. The scissor cut of cotton is somewhat sharper, **20B(4)**. The razor cut of viscose rayon, **20B(5)**, shows much less distortion of the fibre end than the knife cut, **20B(6)**.

Differences between the clean cuts with a razor and the greater distortion of knife and scissor cuts are shown by acetate fibres, **20C(1),(2)**, acrylic fibres, **20C(3),(4)**, and wool, **20C(5),(6)**.

Melting is another deliberate or accidental action, which changes the appearance of a fibre end. The melting of nylon gives a bulbous end to the fibre, but this may be elongated, **20D(1)**, or spherical, **20D(2)**, depending on the distribution of heat. Sometimes, as in the polyester, **20D(3)**, there may be a combination of the two shapes. An acrylic fibre, **20D(4)**, shows a similar form.

When wool is heated it undergoes a combination of chemical change, by decomposition and burning, and physical change, by contraction and melting. The effects are seen as a change to the fibre surface, **20D(5)**, which becomes a more drastic transformation in very severe conditions, **20D(6)**. A bulbous end also forms.

Cellulose fibres, although they normally burn or char when heated, can show some softening similar to melting, as in the viscose rayon fibre, **20E(1)**, which has been held near a flame, although the effects can be more complicated, **20E(2)**, when the fibre is dipped into the flame.

A loose tuft of cotton fibres which has been quickly singed in a spirit lamp is shown in **20E(3)–(7)**. The fibres can take on a quasi-molten appearance, **20E(4)**, or be more severely burnt away, **20E(5)**. Where the fibre is free to contract, bulbous ends can form, **20E(6)**, and these may also become more burnt away, **20E(7)**.

The study of cuts in fibres and fabrics is important for forensic scientists as described in Chapters 44–46. Foos (1993), from the Bayerischen Landeskriminalamtes, has examined cuts in several different fibre types. Polyester fibres cut with a scalpel are shown in **20F(1)**. On the side where the cutting edge makes contact the end of the fibre is slightly rounded, whereas on

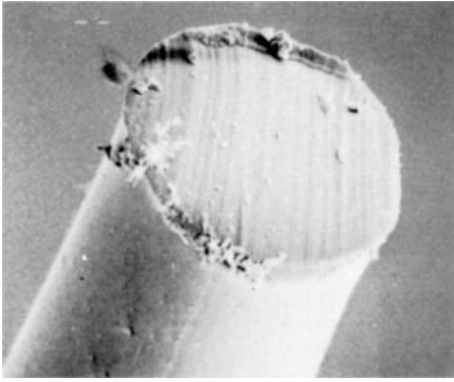
the opposite side material is drawn out. An oblique cut of a polyester fibre, **20F(2)**, clearly shows the marks of the scalpel. The fibre moved as it was being cut. Similar effects are seen in the cutting of acrylic fibres with a scalpel, **20F(3)**.

Piercing of a fabric with a knife gives polyester fibres with more irregularly torn ends, **20F(4)**. A blunt knife can cause acrylic fibres to weld together, **20F(5)**. This test was carried out for comparison with damage in an actual crime, as shown in **44A(5)**. The suspect knife was used to produce the specimen shown in **20F(5)**. The irregular break-up and welding of acrylic fibres in **20F(6)** was produced by an unknown tool, probably a screwdriver. Finally, **20F(7)** shows acrylic fibres cut with scissors, which also causes fibres to weld together.

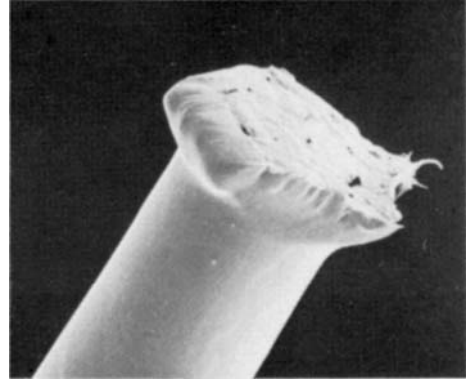
Aramid fibres are extremely difficult to cut. However, in order to obtain cross-sections, they can be cut with a razor after dipping in liquid nitrogen (-196°C). Kevlar 29 is shown in **20G(1)** and Kevlar 49 in **20G(2)**.

In connection with the studies of papermakers' felts, described in Chapter 40, C. Cork and M. A. Wilding of UMIST developed an impact test. A fibre under tension is held in contact with a flat glass anvil and is then impacted by a cylindrical surface of a glass hammer driven by a vibrator. **20G(3)–(4)** show the appearance of a 19 dtex nylon fibre subject to the impact test. There is initial flattening followed by axial splitting and rupture.

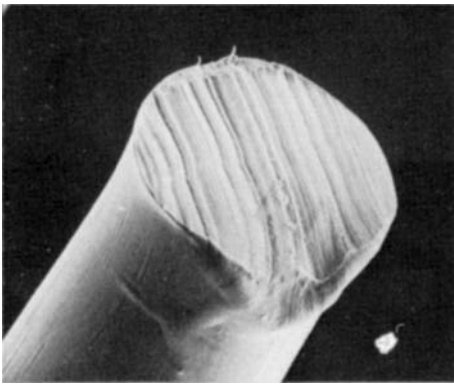
For thermogravimetric analysis, it is necessary to break fibres down into small pieces. As an incidental result, this gives a way of studying the forms of breakdown. Sharma *et al* (1996) have tested unretted flax fibres, which were scutched and hackled from sulphur dioxide treated green straw, and water and enzyme retted fibres from Belgium. The samples were prepared in three ways: by cutting to less than 1 mm length with serrated scissors; by milling in a cyclotec mill to pass through a 0.5 mm sieve; and by freezing in liquid nitrogen for three minutes, followed by grinding in the mill. As seen in **20H(1)–(6)**, there are appreciable differences in the size of particles depending on the method of preparation. The mean fibre length ranged from 2.5 mm for the cut unretted sample to 10.7 mm for the freeze-ground water-retted material. Freeze-grinding causes shearing of the fibres and produces more fine fibre dust. The fibre ends, **20I(1)–(6)**, also differ. Scissor marks can be seen in the cut fibres, whereas the milled fibres had rounded ends. The freeze-ground fibres had deep axial splits.



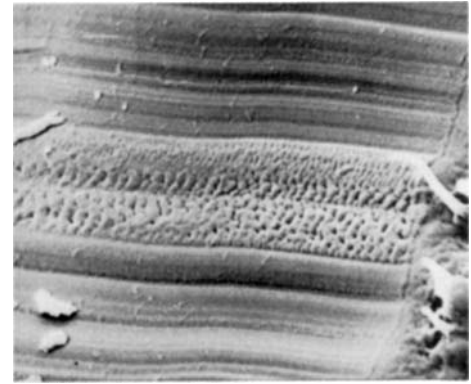
1

5 μm 

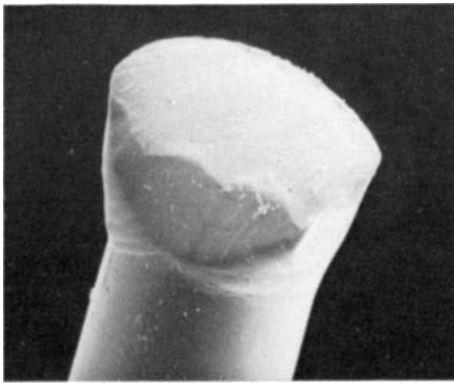
2

10 μm 

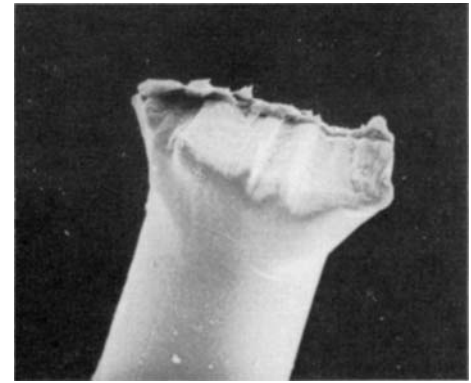
3

5 μm 

4

2 μm 

5

5 μm 

6

10 μm

Plate 20A — Cutting of nylon and polyester fibres.

(1) Nylon cut with a razor. (2) Nylon cut with a knife. (3),(4) Nylon cut with a razor. (5) Polyester cut with a razor. (6) Polyester cut with scissors.

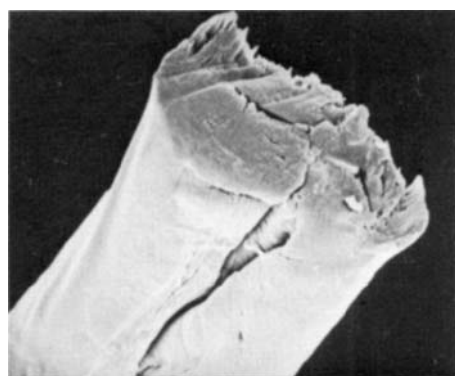
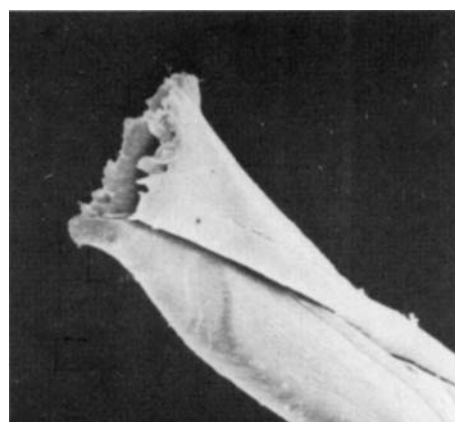
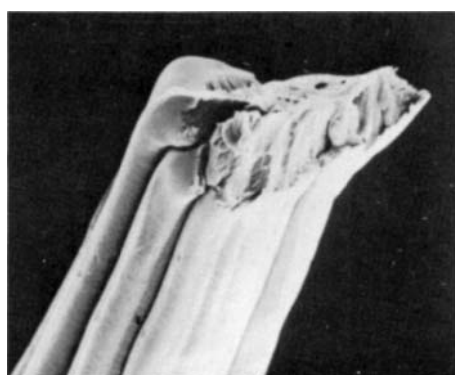
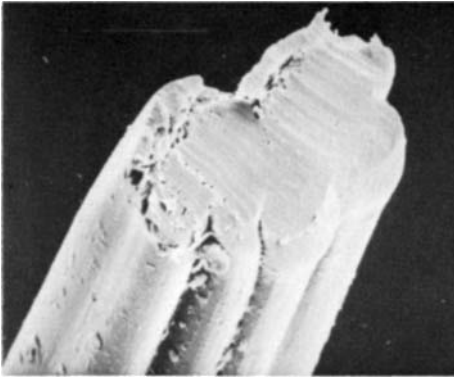
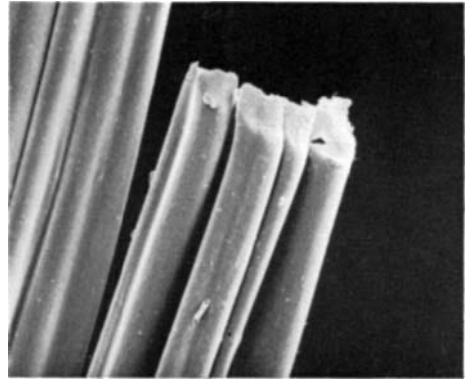
1 |-----| 5 μ m2 |-----| 5 μ m3 |-----| 5 μ m4 |-----| 5 μ m5 |-----| 5 μ m6 |-----| 5 μ m

Plate 20B — Cutting of cellulose fibres.

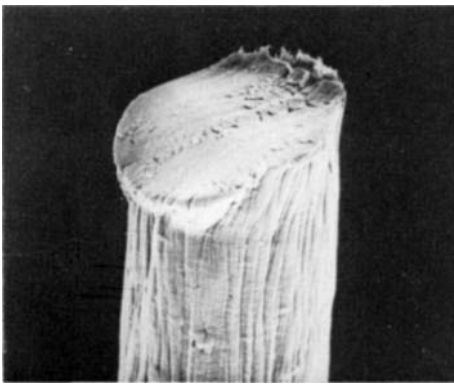
(1), (2) Cotton cut with a razor. (3) Cotton cut with a knife. (4) Cotton cut with scissors. (5) Viscose rayon cut with a razor. (6) Viscose rayon cut with a knife.



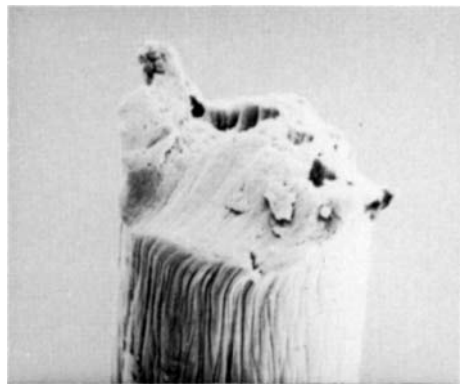
1

5 μm 

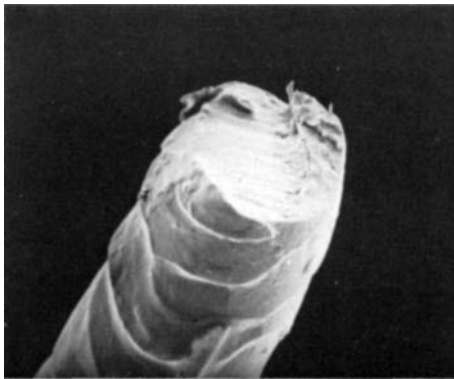
2

10 μm 

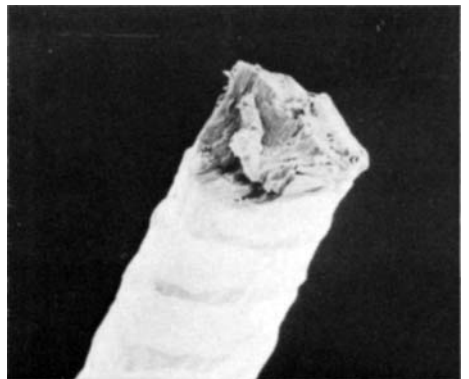
3

5 μm 

4

5 μm 

5

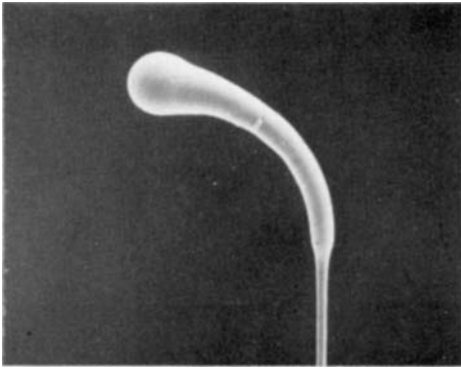
10 μm 

6

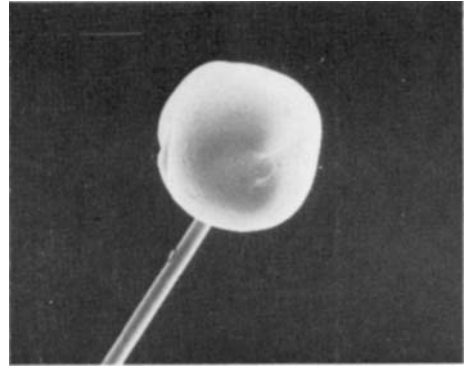
10 μm

Plate 20C — Cutting of acetate, acrylic and wool fibres.

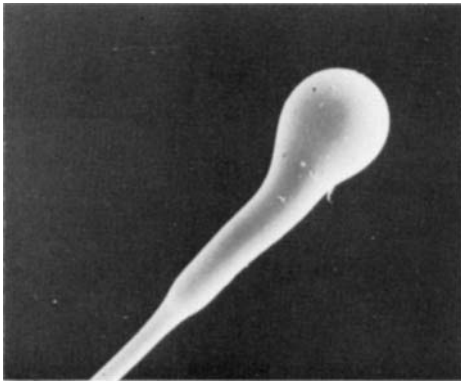
(1) Secondary acetate cut with a razor. (2) Secondary acetate cut with a knife. (3) Courtelle acrylic fibre cut with a razor. (4) Courtelle acrylic fibre cut with scissors. (5) Wool cut with a razor. (6) Wool cut with scissors.



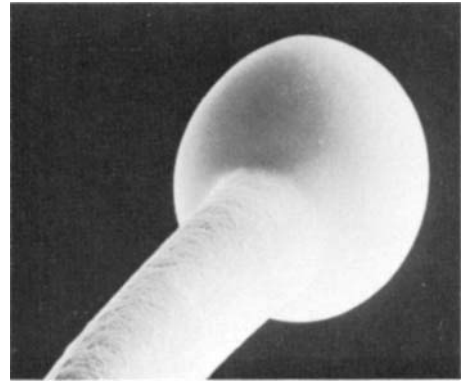
1

|—| 100 μm 

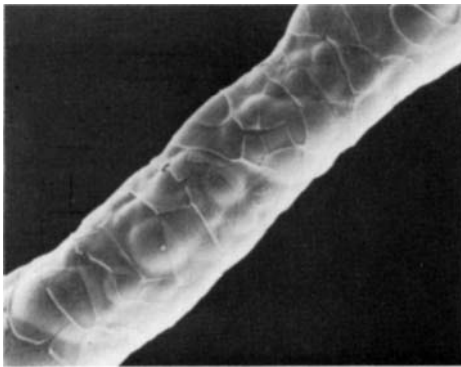
2

|—| 100 μm 

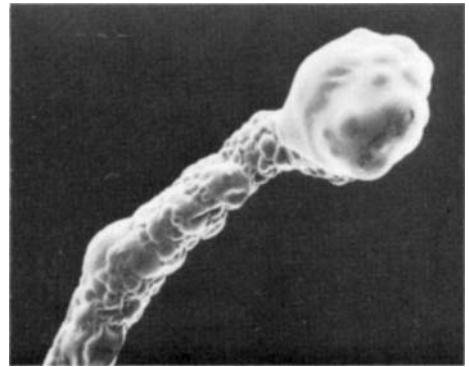
3

|—| 100 μm 

4

|—| 50 μm 

5

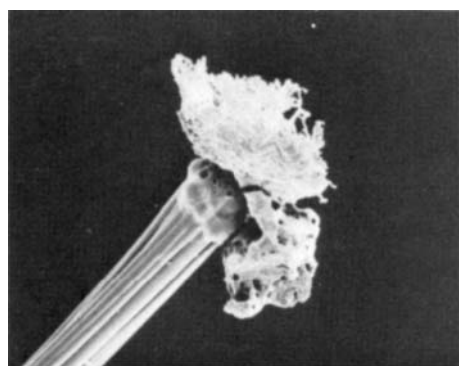
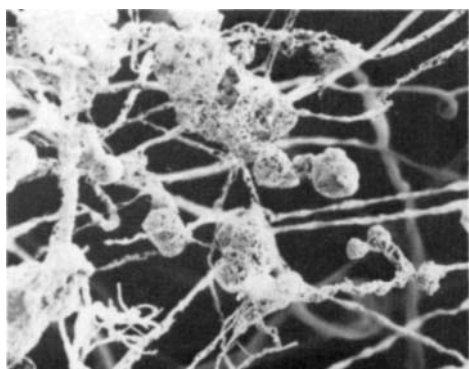
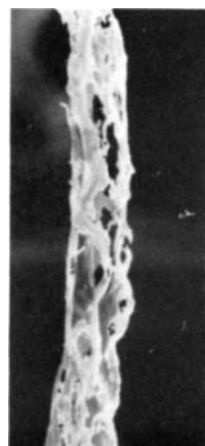
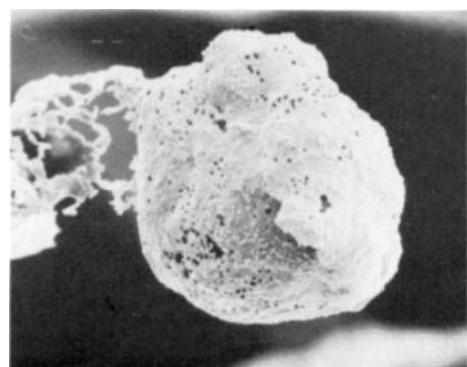
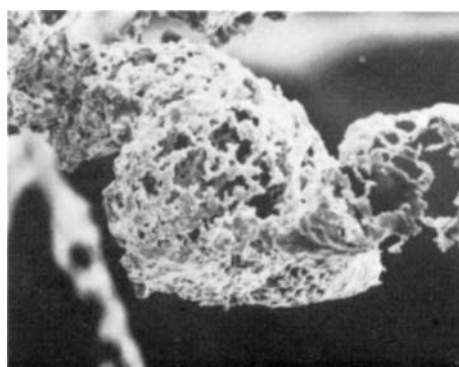
|—| 20 μm 

6

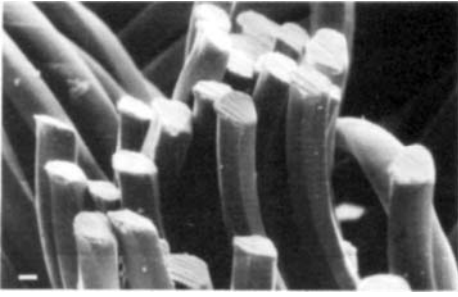
|—| 50 μm

Plate 20D — Melting of fibre ends.

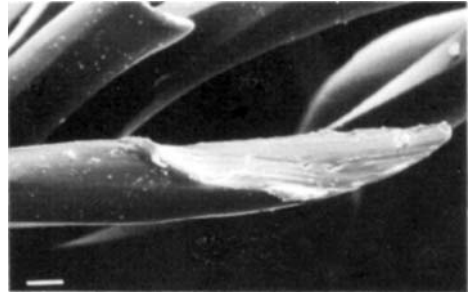
(1) Nylon held near a flame. (2) Nylon quickly dipped into a flame. (3) Polyester held near a flame. (4) Courtelle acrylic fibre held near a flame. (5), (6) Wool drawn through a flame.

1 |—| 5 μm 2 |—| 20 μm 3 |—| 50 μm 4 |—| 10 μm 5 |—| 5 μm 6 |—| 5 μm 7 |—| 5 μm **Plate 20E — Effect of heat on cellulose fibres.**

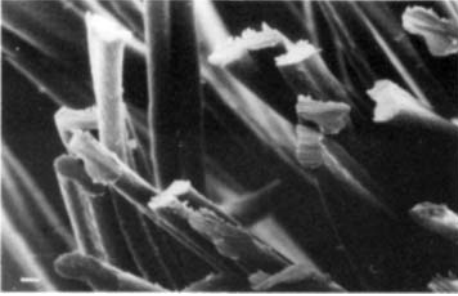
(1), (2) Viscose rayon fibre dipped in a flame. (3)-(7) Tuft of cotton singed in spirit lamp flame.



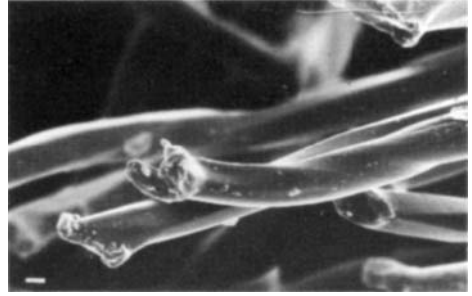
1



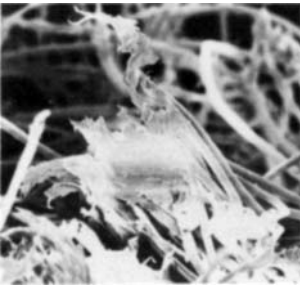
2



3



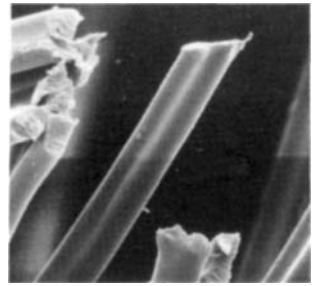
4



5



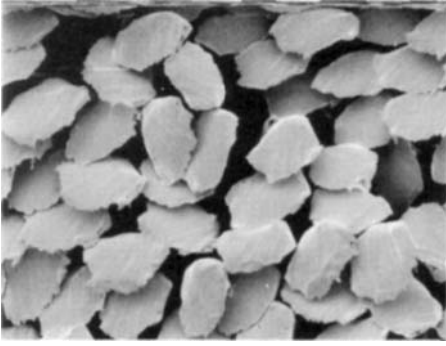
6



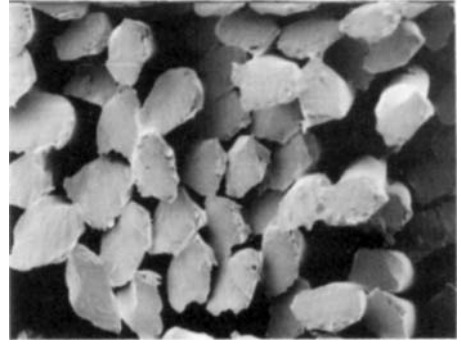
7

Plate 20F — Cutting of fibres, courtesy of Karlheinz Foos, Bayerischen Kriminalamtes.

(1) Polyester fibres cut with a scalpel. (2) Oblique cut of polyester fibre with a scalpel. (3) Acrylic fibres cut with a scalpel. (4) Polyester fibres pierced with a knife. (5) Acrylic fibres welded together by a blunt knife. (6) Welding of acrylic fibres by an unknown tool. (7) Acrylic fibres cut with scissors.



1



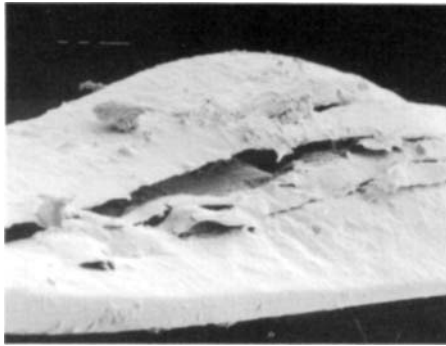
2



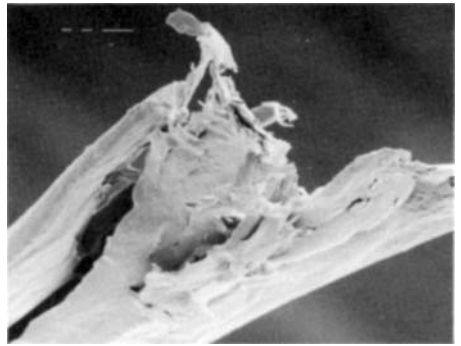
3



4



5



6

Plate 20G — Cuts of Kevlar fibres after cooling to -196°C .

(1) Kevlar 29. (2) Kevlar 49.

Impact on 18 dtex nylon fibre.

(3) Flattening. (4),(5) Axial splitting. (6) Rupture.

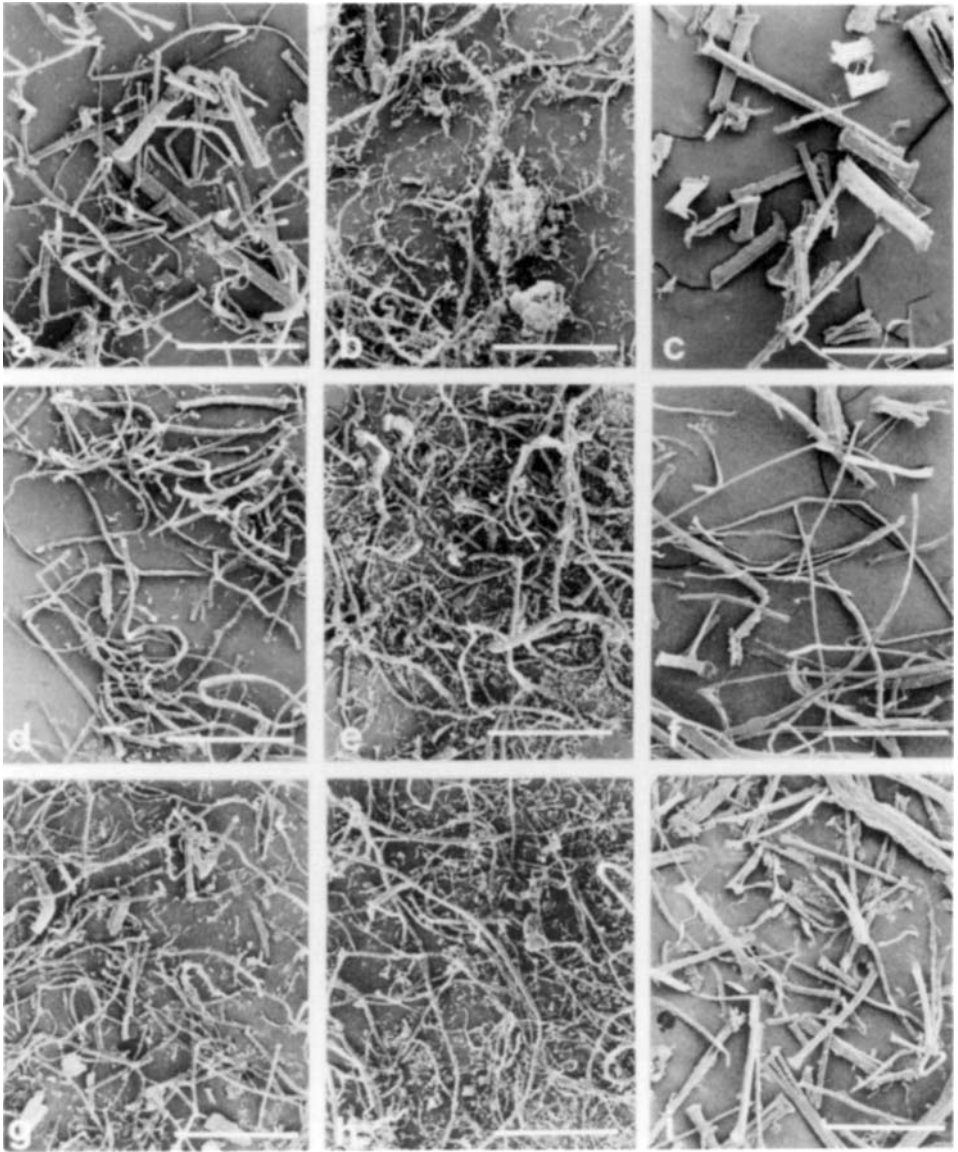


Plate 20H — Flax fibres prepared for thermogravimetric analysis, Sharma et al (1996).

[a] Unretted milled. [b] Unretted freeze-ground. [c] Unretted cut. [d] Enzyme-retted milled. [e] Enzyme-retted freeze-ground. [f] Enzyme-retted cut. [g] Water-retted milled. [h] Water-retted freeze-ground. [i] Water-retted cut.

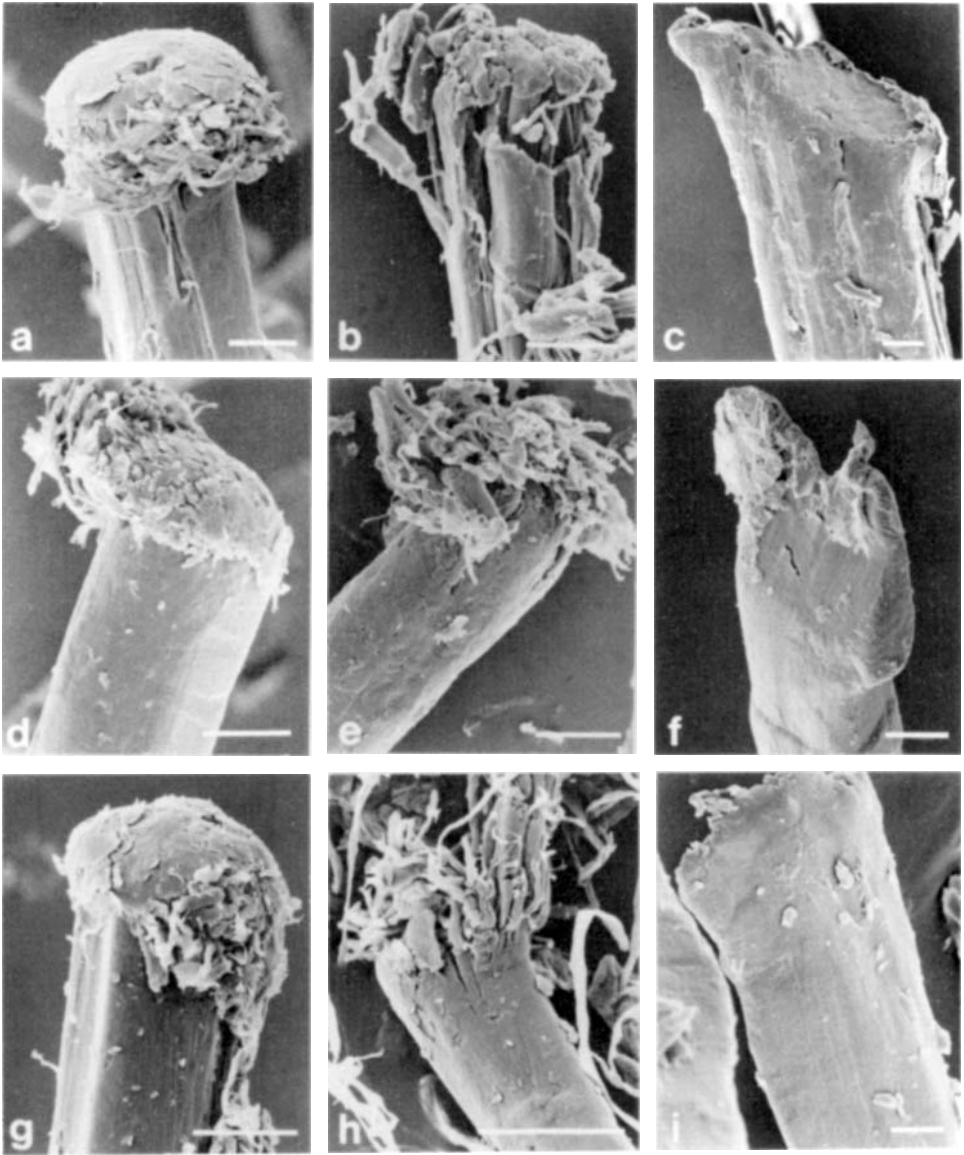


Plate 201 — Ends of flax fibres prepared for thermogravimetric analysis, Sharma et al (1996).

[a] Unretted milled. [b] Unretted freeze-ground. [c] Unretted cut. [d] Enzyme-retted milled. [e] Enzyme-retted freeze-ground. [f] Enzyme-retted cut. [g] Water-retted milled. [h] Water-retted freeze-ground. [i] Water-retted cut.

21

MISCELLANY

This chapter contains a miscellaneous collection of breaks which have been found in laboratory tests either of fibres of specialized interest or in special conditions.

Apart from cotton, most plant fibres in commercial use as textile or cordage fibres have a more highly oriented molecular arrangement, with fibrils following helical paths at an angle of about 10° to the axis, and they are multicellular. Their tensile breaks tend to be granular across the fibre, but show evidence of the separate cells. This is illustrated for jute, **21A(1)**, **(2)**, and flax, **21A(3)**. A hollow, unicellular seed fibre shows a granular break straight across the fibre, **21A(4)**.

Silk is a natural fibre which is spun from a solution extruded by the silkworm. The tensile breaks, **21A(5)**, **(6)**, are granular and similar to those of the man-made fibres spun from solution and shown in Chapter 8.

Hollow polyester fibres may show a tensile break, **21B(1)**, which is a modified form of the normal ductile failure; but we also find examples in which two separate fractures are joined by an axial split, **21B(2)**.

The thermally resistant meta-aramid fibre, Nomex, shows rather unusual breaks, which appear to be intermediate between granular and ductile, **21B(3)**, **(4)**.

PVC fibres are made in France and used to a limited extent: they are solution-spun fibres, similar to other vinyl fibres such as the acrylics, and the form of break is similar, **21B(5)**.

Polytetrafluorethylene is better known as a bulk plastic or as a coating, but it is made into fibres for specialized industrial purposes. It is an extremely inert material; there are no solvents for solution-spinning; and it decomposes at a high temperature as it begins to soften, prior to the melting which would occur if the decomposition had not occurred. These difficulties make it necessary to spin by extrusion of a dispersion, followed by sintering to hold the fibre together. The tensile break shows many separate fibrillar ruptures, **21B(6)**. This may be another example of independent fibrillar failure, type 6 of Fig. 1.2, otherwise only found in wet cotton, as described in Chapter 9. Weak cohesion of separate elements of the dispersion, even after sintering, would explain this.

Monvelle is a bicomponent fibre in which one half is nylon and the other half is an elastomeric segmented polyurethane. Differential contraction makes this a helically crimped fibre. The snap-back into a helical tangle after break, **21C(1)**, makes detailed examination of the broken end difficult; but it is possible to see that each half has broken with its own characteristic form, **21C(2)**, **(3)**. The nylon shows the usual ductile failure, described in Chapter 5, while the elastomer shows a brittle failure, as found in single-component elastomeric fibres, **4C(4)**–**(6)**. The breaks of the two parts are sometimes separated along the fibre.

A different sort of bicomponent fibre, used as a high-performance fibre in composites, consists of silicon carbide which has been vacuum deposited on a tungsten core. The diameter of the fibre is $100\ \mu\text{m}$, and of the core is $20\ \mu\text{m}$. A single-fibre tension test in air causes brittle failure, as shown in **21C(4)**, initiated at a surface defect at a strain of about 0.6%, corresponding to a stress of 2.1 GPa. However, when the fibre was embedded in epoxy resin, the break propagates radially outwards, following initiation at the tungsten core, as shown in **21C(5)** for a fibre which broke at 1.0% strain or about 3.5 GPa stress. In some instances, as seen in **21C(6)**, the break originated at a defect between the silicon carbide and the tungsten core; this was a source of weakness, with the failure occurring at 0.8% strain, 2.8 GPa stress.

The effect of bending on the highly oriented, para-aramid fibre, Kevlar, is shown in **21D**. In a loop test around a wire, giving an apparent bending strain of 4.7%, the strength had fallen to 47% of the value for a straight fibre, but the broken fibre, **21D(1)**, was very similar to the tensile breaks, shown in Chapter 7, with long axial splits.

In one set of bending fatigue experiments, a short length (2.5 mm) of the Kevlar fibre was buckled by decreasing the distance between the grips by 30%. It was then oscillated about this mean value, between 20% and 40% contraction. The smooth buckling curve soon changes to a sharp kink, but even after 1 week at 50 Hz (over 30 million cycles) the fibre had not broken, **21D(2)**. A subsequent tensile break of such a fibre shows that it has split into fibrils in the kinked region, **21D(3),(4)** thus relieving the strain.

Flex fatigue of Kevlar, by pulling the fibre backwards and forwards over a pin which is free to rotate, so that the surface wear reported in Chapter 14 does not occur, leads to failure with thinning, fibrillation and some flattening, **21D(5)**. Rotation over a pin gives a typical multiple splitting failure, **21D(6)**.

In the biaxial rotation fatigue test of nylon or polyester fibres, discussed in Chapter 13, it sometimes happens that break occurs after relatively few cycles, before the twisting has reached a steady state. These breaks are called direct breaks, and they occur when the angle of wrap round the pin is too large, so that a high torque is needed to overcome the external and internal friction. One might expect a simple twist break to occur, but this is not so. Complicated forms of deformation occur, and these are probably associated with the influence of torque on a fibre which is weakened and softened by the repeated bending and perhaps by frictional heating. The motion in the pin at the beginning of a test can be jerky, as a fibre rolls along and then slips.

The first effect is the formation of bulbous zones at positions of high torque where the fibre leaves the pin, **21E(1)**. Sometimes these appear at intervals along the fibre, **21E(2)**, but the reasons for this are not understood. The structural changes within the fibre can be seen by examination in polarized light microscopy, **21E(3)**. The fringes at A and B are typical of undamaged fibres, and are due to increasing optical path difference with thickness in a birefringent fibre. The way in which the fringes swing round at C and D, to indicate a lower optical path difference in a thicker fibre cross-section, means that the birefringence must be much reduced. The fibre has softened, disoriented and contracted.

The final failure can show at least three different forms: 'wagon-wheel' cavitation, **21E(4)**; pinching off under torque, **21E(5)**; and spreading out, **21E(6)**.

Calcium alginate fibres are used in medical dressings. Their breaks, seen in **21F(1)–(3)**, have a granular form, with evidence of failure at internal faults in the fibre. Thistledown is a natural fibre, made up of a collection of tubular structures, **21F(4)**. These easily fibrillate, **21F(5)**. Rupture is shown in **21F(6)**.

Tencel from Courtaulds is a new lyotropic cellulose fibre, which is having a significant market impact. Its tensile breaks were shown in **8E**. As shown in **21F(7),(8)**, it easily fibrillates. Although this might be a disadvantage in some circumstances, it is a property that can be exploited favourably, as described in Chapter 23.

BACTERIAL FIBRES by J. J. Thwaites and N. H. Mendelson

Bacterial thread is a multifilament fibre formed from cultures of a cell-separation-suppressed mutant of the Gram-positive bacterium *Bacillus subtilis*. The bacteria, which are normally rod-shaped, 0.8 μm in diameter and up to 4 μm in length, are grown as cellular filaments up to 1 mm in length, producing in a Petri dish an aggregation that resembles a random textile web. Thread is produced by lifting part of the web from the culture by means of a wire hook. The surface tension has the effect of a die and other filaments are drawn radially into a fibre as the hook is raised. The filaments are close-packed and highly aligned parallel to the fibre axis. The fibre has a circular cross section and, given a uniform web, is of constant diameter over lengths up to about 100 mm. For a fibre of diameter 100 μm the cross section contains about 15 000 filaments; a specimen of length 100 mm contains therefore almost 10^9 cells, Thwaites and Mendelson (1985).

Bacterial thread can be tested in tension in the same way as other fibres. No interfilament slippage is observed; it is clear that the cells adhere strongly to each other, even in very humid atmospheres. The material shows typical polymer behaviour of relaxation and recovery; it is stiff and brittle when dry but ductile at high relative humidity, with initial modulus smaller by a factor of about 1000. Bacterial cells have no internal structure so that the material involved is the cell wall, which occupies about one-fifth of the fibre cross section. The load bearing polymer of the wall, peptidoglycan, is a polysaccharide with short peptide side chains. It accounts for half the wall mass. There is no evidence of crystallinity. The measured initial modulus is about 20 GPa when dry, its tensile strength is about 300 MPa and its extensibility <0.5%. At high relative humidity the extensibility can be as high as 70% and the tensile strength falls to about 15 MPa, Thwaites and Surana (1991a).

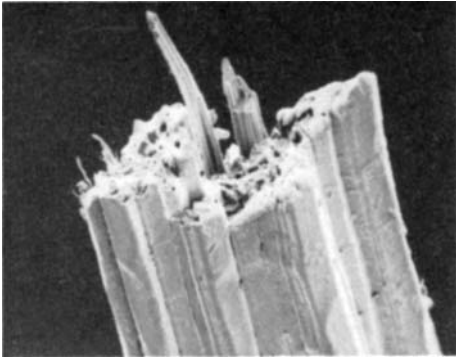
21G(1), a scanning electron micrograph, shows the fracture cross section of a bacterial thread as first drawn. The filaments are aligned and appear not to have collapsed during drying but have deformed into approximately hexagonal shape. **21G(2),(3)** show similar cross sections for bacterial thread from which the residual culture medium has been removed by

washing in water, **21G(2)**, and for which the walls have been attacked by lysozyme, **21G(3)**, Thwaites *et al* (1991b). The effect of washing is merely to raise the 'transition' relative humidity by 18% without changing the measured parameters. Surprisingly the properties are not changed by lysozyme attack, even though it produces substantial circumferential cracks in the fibre surface. Lysozyme preferentially cleaves the cross walls between adjacent cells in a filament. This accounts for the cracks. It breaks the glycosidic bonds of the peptidoglycan backbone. The unchanged tensile properties indicate respectively how strong the lateral cell adhesion is, and that, although the cell wall is amorphous, there is order in the peptidoglycan, with its backbone lying on average in a circumferential direction in the cell wall.

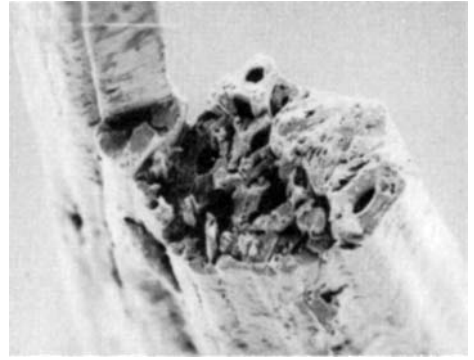
Both peptidoglycan and the other major cell wall polymer in *Bacillus subtilis*, teichoic acid, carry ionizable groups that collectively result in a highly electro-negative material. Counter-ions must neutralize the majority of these charges to maintain the integrity of cell wall. Many different ions can serve to do so, thus cell wall can act as a complex ion exchanger. Ion binding can lead to nucleation of crystallization within the interior and on the cell wall surface. Such processes are thought to be responsible for the geochemical deposition of some minerals.

Mineralization of cell walls can also be achieved under laboratory conditions and large fibre-like structures called bionites have been made, Mendelson (1992). Chloride salts of iron, copper and calcium when added directly to the culture medium containing a *Bacillus subtilis* web of filaments give rise to mineralized fibres when the web is later drawn from the solution. Bionites have also been produced by hydrating bacterial thread in ion solutions and then redrawing, and by transferring a filament web from its culture medium into an ion solution prior to drawing. The structure and material properties of bionites differ depending upon the composition of the inorganic solid. All of them resemble bacterial thread in having their bacterial filaments aligned along the fibre axis. Bionites are generally shorter and of increased diameter compared to threads produced from similar cultures.

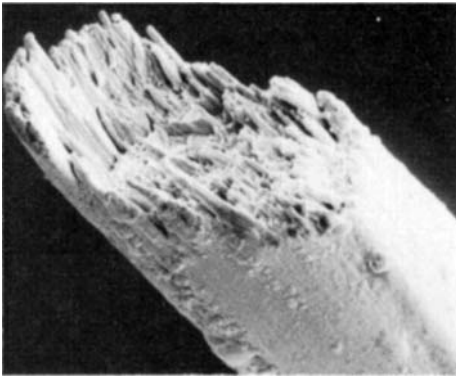
21G(4) shows a SEM image of a crack edge cross section obtained from a bionite produced by addition of FeCl_3 to the growth medium. The inorganic solid present is Fe_2O_3 . Mineralization throughout is evident. Bundles of cell filaments can be resolved in the bionite interior as well as on its surface. Ferric bionites are brittle structures that spontaneously crack when stored at low relative humidity (<30% rh), Mendelson (1992). **21G(5)** shows the surface of a KDP bionite obtained by suspension of a filament web in a 1 M solution of potassium dihydrophosphate (KDP). The fibre axis is aligned with that of the long hollow tube crystals. All the crystals were produced during the drying process after drawing. Their upper ends begin in the bionite interior. The open ends point downwards in the direction of fluid drainage during drying. The crystal composition (KDP) was determined by comparison of its X-ray diffraction powder pattern with a known KDP spectrum, Mendelson (1994). **21G(6)** shows the fractured surface of a bionite produced by first suspending a filament web in 1 M CaCl_2 , drawing the structure and immediately resuspending it in a solution of 1 M KDP before final drawing. Individual cell filaments that lie along the fibre axis are coated with mineral. The composition of the inorganic solid has not yet been determined, Mendelson (unpublished).



1

|—| 20 μm 

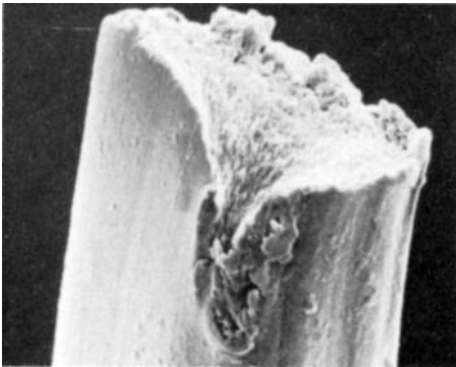
2

|—| 10 μm 

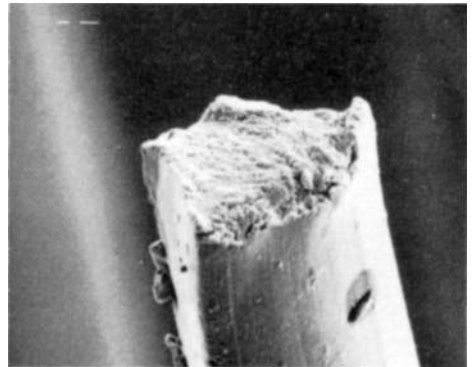
3

|—| 2 μm 

4

|—| 5 μm 

5

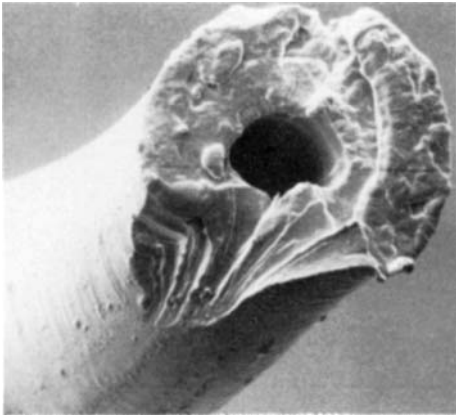
|—| 2 μm 

6

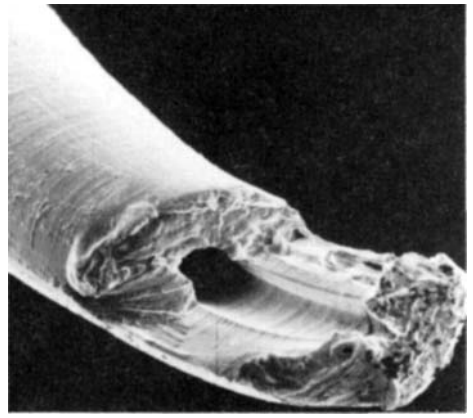
|—| 5 μm

Plate 21A — Tensile breaks of some natural fibres.

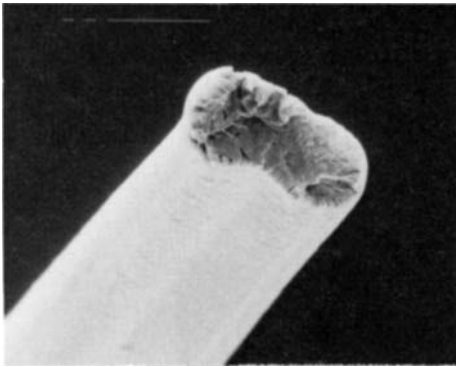
(1), (2) Jute. (3) Flax. (4) A seed fibre from the Iranian desert. (5), (6) Cultivated silk.



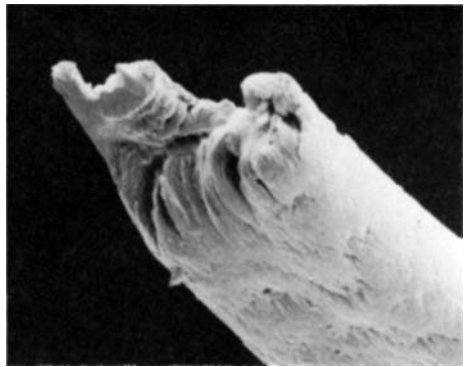
1

|—| 10 μm 

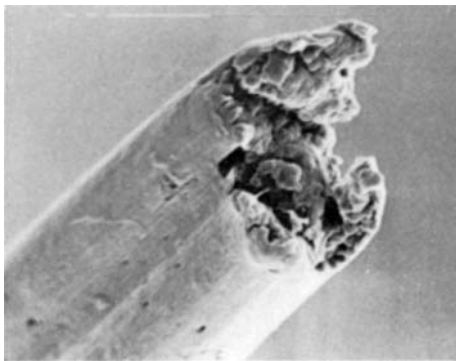
2

|—| 5 μm 

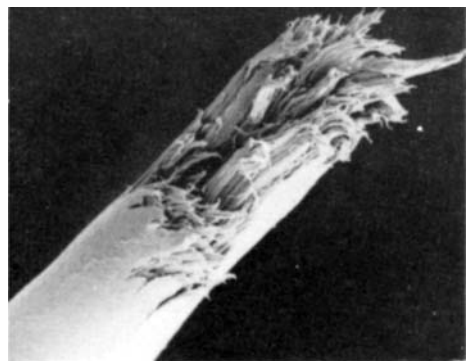
3

|—| 5 μm 

4

|—| 5 μm 

5

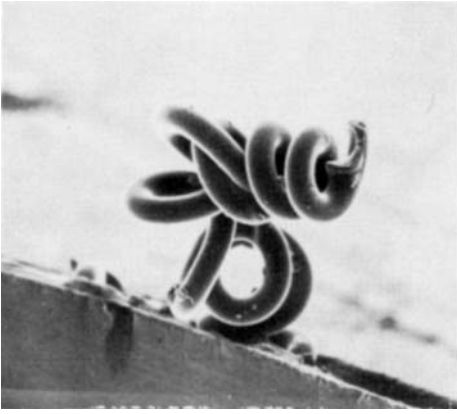
|—| 5 μm 

6

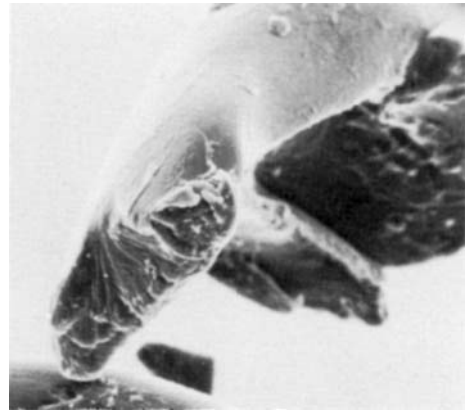
|—| 10 μm

Plate 21B — Tensile breaks of some man-made fibres.

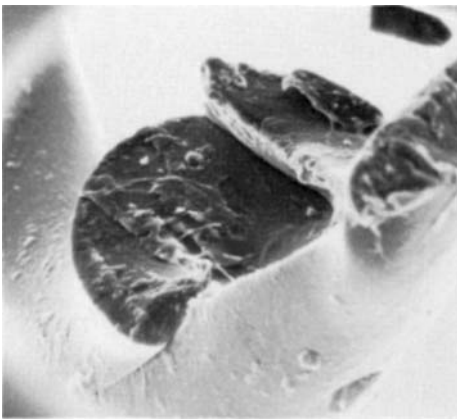
(1), (2) Hollow polyester fibres. (3), (4) Nomex meta-aramid fibre. (5) Rhovyl PVC fibre. (6) Polytetrafluorethylene (PTFE), Teflon fibre.



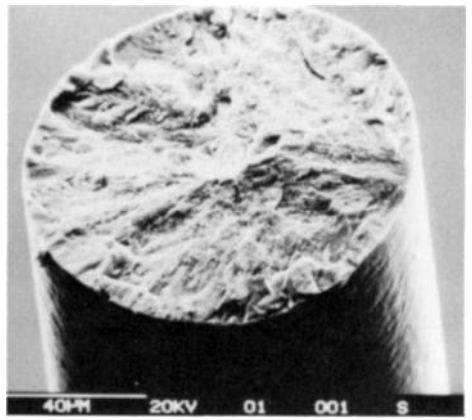
1

|—| 100 μm 

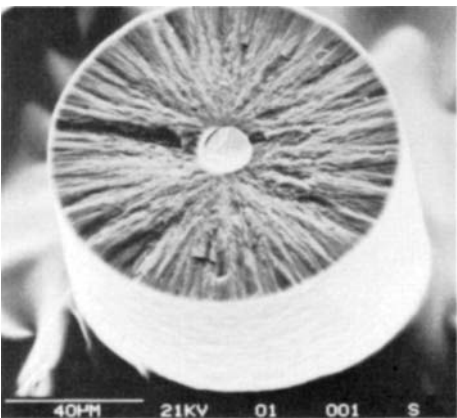
2

|—| 10 μm 

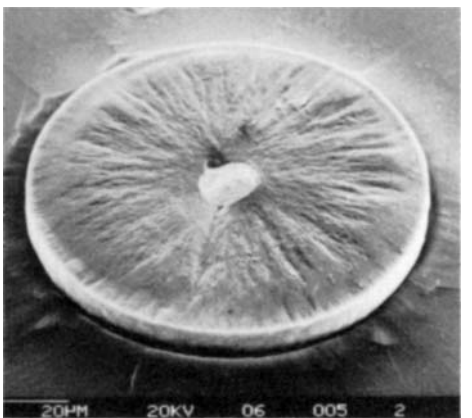
3

|—| 10 μm 

4



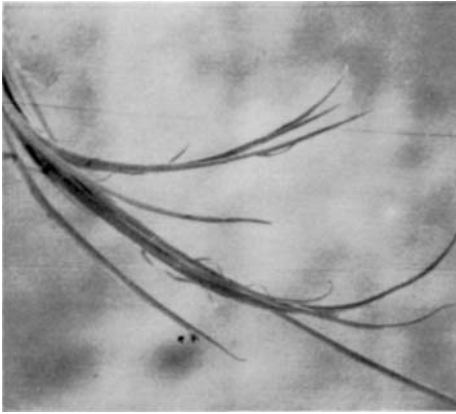
5



6

Plate 21C — Tensile breaks of bicomponent fibres.

(1)–(3) Monvelle bicomponent fibre. (4)–(6) Silicon carbide fibre (by courtesy of M. G. Bader and D. A. Clarke, University of Surrey).



1



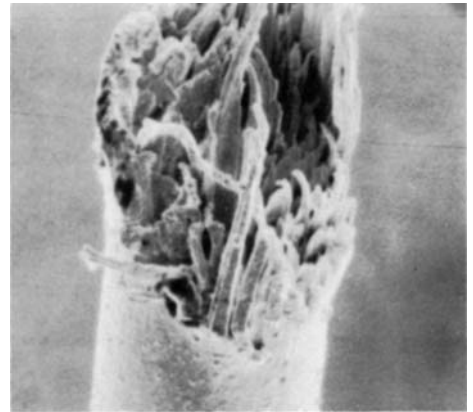
2

|-----| 10 μm



3

|-----| 5 μm

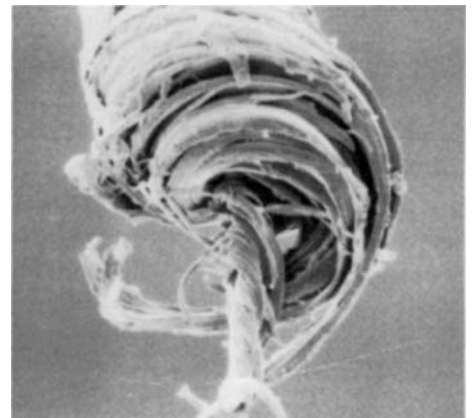


4

|-----| 5 μm



5

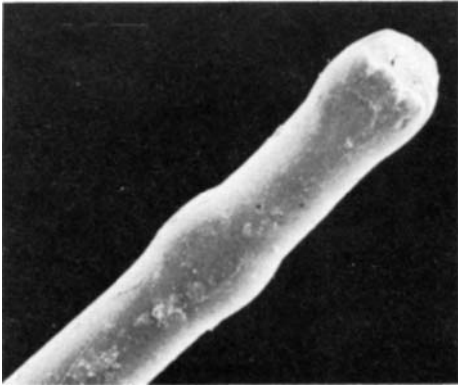


6

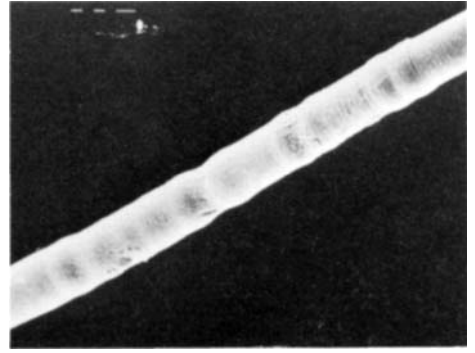
|-----| 5 μm

Plate 21D — Flexural failures of Kevlar.

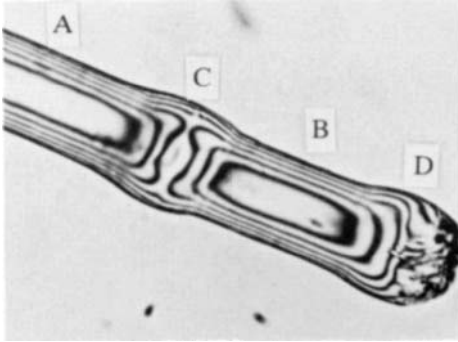
(1) Broken in a loop tensile test around a wire with an apparent bending strain of 4.7%, with 47% loss of strength. (2) After 30×10^6 cycles of buckling between 20% and 40% contraction. (3), (4) Opposite ends of tensile break of Kevlar after repeated buckling, as in (2). (5) Flex fatigue over a rotating pin, failed after 111 000 cycles with a nominal bending strain of 2.14% and a tension of 0.5 N/tex. (6) Fatigue by rotation over a pin with a weight attached to the free end, failed after 11 000 cycles, a nominal bending strain of 7.7% and a tension of 0.04 N/tex.



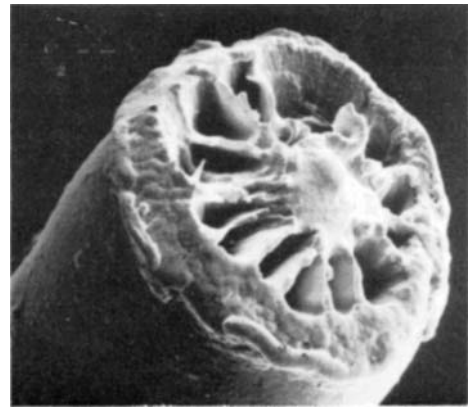
1

 20 μm


2

 50 μm


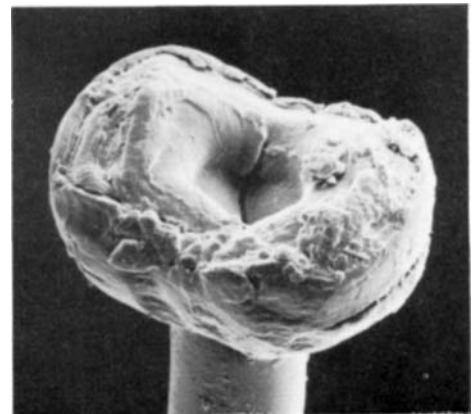
3



4

 5 μm


5

 5 μm


6

 10 μm

Plate 21E — 'Direct' breaks of nylon in biaxial rotation fatigue tests.

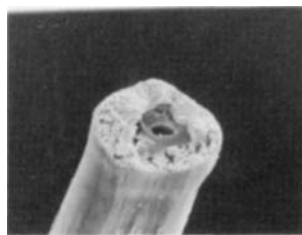
(1) Bulbous forms seen in SEM. (2) Bulbous forms appearing at intervals along a fibre. (3) Polarization fringes in optical microscopy. (4)–(6) Forms of break.



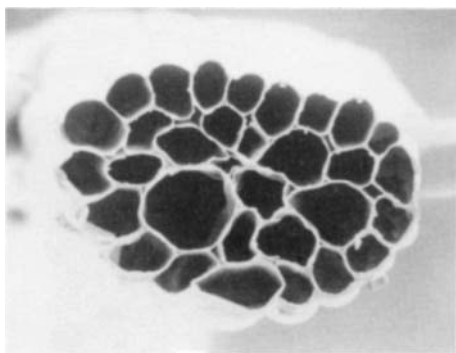
1



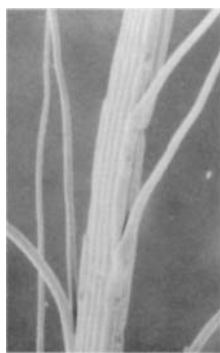
2



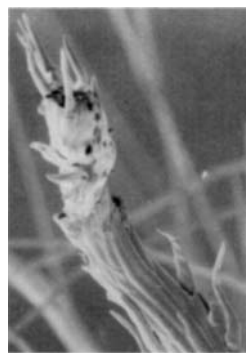
3



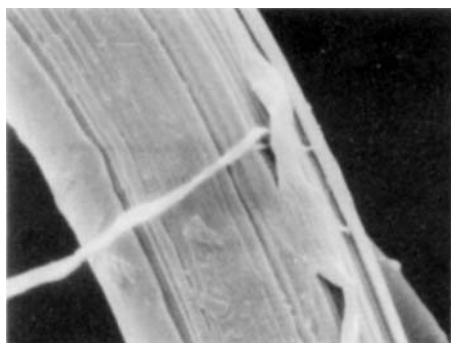
4



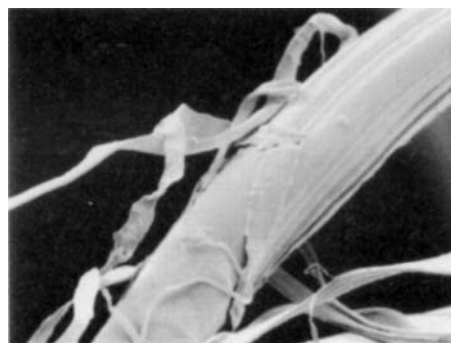
5



6



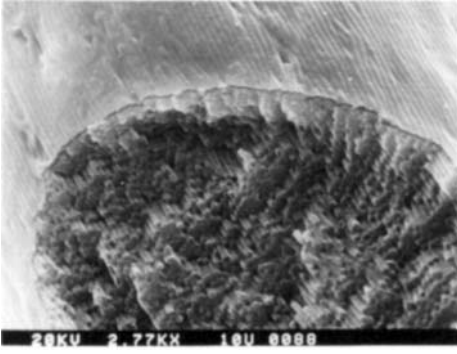
7



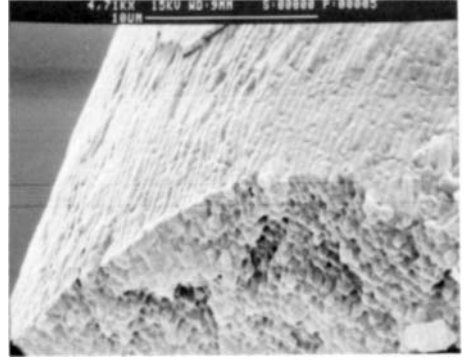
8

Plate 21F — New and unusual fibres.

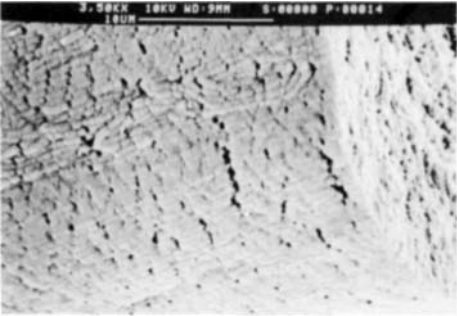
(1)–(3) Breaks of calcium alginate fibres. (4)–(6) Thistle-down. (7), (8) Fibrillation of Tencel.



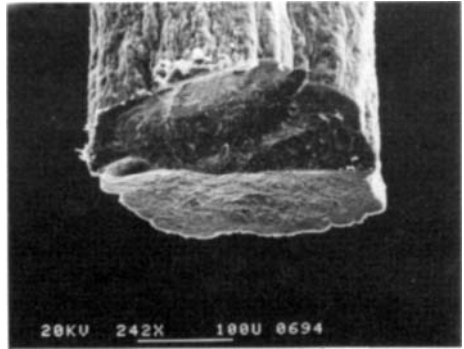
1



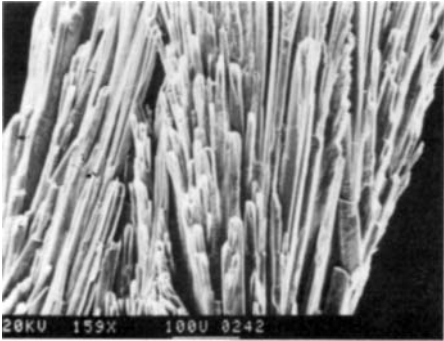
2



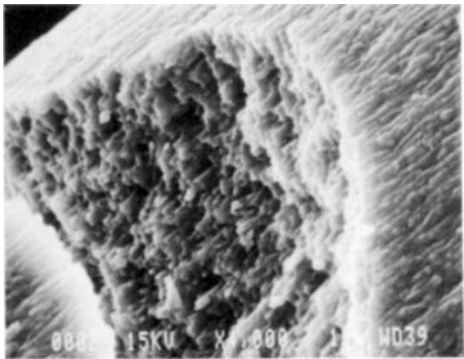
3



4



5



6

Plate 21G — Bacterial threads.

(1) Fracture of drawn bacterial thread. (2) Fracture of thread washed in water. (3) Fracture of thread attacked by lysozyme. [Bars are 10 μm .] (4) Crack edge of ferric bionite [Bar = 100 μm .] (5) Surface of KDP bionite [Bar = 50 μm .] (6) Fracture of a bionite [Bar = 1 μm .] Micrographs reproduced by permission of American Society for Microbiology, American Association for Advancement of Science and Material Research Society.